Quantitative Finance

ISSN: (Print) (Online) Journal homepage: www.tandfonline.com/journals/rquf20

An orthogonal expansion approach to joint SPX and VIX calibration in affine stochastic volatility models with jumps

Thomas K. Kloster & Elisa Nicolato

To cite this article: Thomas K. Kloster & Elisa Nicolato (2025) An orthogonal expansion approach to joint SPX and VIX calibration in affine stochastic volatility models with jumps, Quantitative Finance, 25:1, 63-89, DOI: 10.1080/14697688.2024.2433142

To link to this article: https://doi.org/10.1080/14697688.2024.2433142

Published online: 16 Dec 2024.

Quantitative Finance, 2025
Vol. 25, No. 1, 63–89, https://doi.org/10.1080/14697688.2024.2433142

An orthogonal expansion approach to joint SPX and VIX calibration in affine stochastic volatility models with jumps

THOMAS K. KLOSTER* and ELISA NICOLATO

Department of Economics and Business Economics, Aarhus University, Fuglesangs Allé 4, Aarhus V, 8210, Denmark

(*Received 22 December 2023; accepted 9 November 2024*)

We discuss the joint calibration to SPX and VIX options of an affine Stochastic Volatility model with Jumps in price and Jumps in volatility (the SVJJ model). Conventionally, the SVJJ model assumes exponential jumps in the variance process, leaving the potential benefits of more flexible jump distributions unexplored. The purpose of our study is twofold. First, we show that choosing the gamma distributions for the jumps in variance significantly improves the performance of the joint calibration. However, this improvement comes at the cost of increased computational time. Second, we mitigate this loss of tractability by constructing novel approximations to option prices based on orthogonal polynomial expansions. Unlike the classical method of selecting an explicit reference density, our approach generalizes to all densities with explicit Laplace transform. We apply this methodology to the SVJJ model with gamma jumps and we find that the proposed price expansions achieve the same accuracy as exact transform inversion formulas while requiring only a fraction of the computational time.

Keywords: Affine jump-diffusion; Orthogonal polynomials; Jump distributions; Joint calibration; Transform inversion; Option pricing

JEL Classifications: C02, C63, C65, G10, G13

1. Introduction

The CBOE's volatility index, or simply the VIX, is a widely recognized indicator of market's expectation for future equity volatility. Following the CBOE (2023) white paper, the computation of the VIX is based on a weighted average of put and call options written on the S&P500 index (SPX options). More precisely, the options are selected so that—under the assumption of continuous SPX paths—the squared of the VIX is an approximate replication of the fair swap rate of a 30-days variance swap. As such, the VIX provides a model-free risk-neutral estimate of the 30-days ahead market volatility. To satisfy the appetite of market participants towards pure volatility exposure, the CBOE introduced the first exchange-traded VIX futures contract in 2004 followed by VIX options two years later. Since then, the market of VIX derivatives has grown rapidly and now constitutes a quarter of the total turnover in derivatives on the SPX index.

The structural connections between the VIX and the SPX index call for valuation models aiming at reproducing the stylized features of both the SPX and the VIX option markets by matching the corresponding implied volatility surfaces as close as possible. A well-known challenge of the joint SPX-VIX calibration problem is to reconcile the very large negative skew of short-term SPX options with the comparatively low levels of VIX implied volatilities, which are further characterized by an upward slope.

Several modeling approaches have been proposed in the literature with many contributions resorting to the inclusion of jumps both in the SPX and the volatility dynamics. Sepp (2008), Lian and Zhu (2013) and Kokholm and Stisen (2015) consider a jump-augmented version of the Heston (1993) model. Bardgett *et al.* (2019) and Pacati *et al.* (2018) look at multi-factor volatility extensions, Maneesoonthorn *et al.* (2017) include self-exciting jumps by using Hawkes processes, and Cont and Kokholm (2013)

*Corresponding author. Email: tkk@econ.au.dk

incorporate jumps in the joint dynamics of the SPX and its implied forward variance swap curve. In a different line of research, a number of authors argue that adequate results may be achieved by utilizing stochastic volatility models based uniquely on continuous paths. Here we mention rough volatility models pioneered by Bayer *et al.* (2016) (see Rømer 2022, Abi Jaber and Li 2024 for the empirical analysis of the calibration performances of numerous rough volatility specifications), path dependent volatility models by Guyon and Lekeufack (2023), and signature-based models by Cuchiero *et al.* (2023). The recent contributions by Bondi *et al.* (2024a, 2024b), however, suggest that adding jumps to the rough stochastic volatility framework is a parsimonious way to simultaneously fit the SPX and VIX implied volatility surfaces.

In this paper we embrace the hypothesis that the dynamics of both the SPX and its volatility exhibit jumps, and we test the SPX-VIX calibration performances for a number of alternative model specifications. Our analysis focuses on a modeling assumption which has received little attention, namely the selection of the jump distribution. Remarkably, in most of the above mentioned models where the variance process exhibits jumps, the canonical choice falls on the exponential distribution, possibly in the interest of parsimony and analytical tractability. One exception is the joint SPX-VIX calibration study conducted by Cont and Kokholm (2013) in a framework where the log-forward variance swap rates are modeled as affine processes. Both Gaussian and double exponential jumps are considered to find that the calibration results are not sensitive to the particular jump specification. In contrast, Nicolato *et al.* (2017) consider affine stochastic volatility models where jumps are added to the variance process and show—via an asymptotic analysis of implied volatility wings—that the pricing of VIX products can be very sensitive to the specific distribution of jumps: Ceteris paribus, different choices for the variance jumps lead to completely different shapes and characteristics of the VIX implied volatilities.

The first purpose of this work is to investigate to which extent the selection of the variance jump distribution impacts the joint SPX-VIX calibration problem within the affine modeling setup. More precisely, we consider the Stochastic Volatility model with Jumps in price and Jumps in volatility (the SVJJ model) from the framework of Duffie *et al.* (2000). The SVJJ setup is appealing as it is flexible enough to provide reasonable calibration results. Yet, the simple dynamics allow us to assess the impact of the variance jump distribution in isolation, without dealing with the effects of further modeling sophistication.

We conduct a series of empirical joint calibrations where we run a horse-race between three distinct SVJJ specifications: the SVJJ-E model, where variance jumps are exponentially distributed, against the SVJJ-G and SVJJ-IG models where variance jumps are distributed respectively according to a gamma and an inverse Gaussian distribution. The SVJJ-E model is the specification originally suggested by Duffie *et al.* (2000) and has already been empirically investigated, e.g. in Kokholm and Stisen (2015). At the best of our knowledge, other jump distributions have not been examined so far. We consider daily SPX and VIX option prices as well as VIX futures spanning intervals of six weeks in the years 2018, 2019 and 2020. The winner of the calibration race is the SVJJ-G model which consistently outperforms the SVJJ-E and SVJJ-IG counterparts in each of the examined periods. Most of the improvement comes from a better fit to VIX products. Under SVJJ-G dynamics, the VIX implied volatility errors are on average ca. 20% and 40% smaller than those produced by the SVJJ-E and the SVJJ-IG models. Similarly, the errors for VIX futures prices are on average ca. 30% and 40% smaller than in the SVJJ-E and SVJJ-IG specifications. All in all, our analysis shows that the choice of the jump distribution, an aspect of the modeling concoction which is often considered secondary, can significantly impact the joint calibration performance.

The increased flexibility, however, is not entirely free of unpleasant implications. The Fourier pricing procedure under SVJJ-G dynamics is about 10 times slower than in the standard SVJJ-E specification, as the relevant transforms contain an integral expression that needs to be evaluated numerically. This computational setback motivates the second purpose of this work: to develop efficient and robust option price approximations based on orthogonal polynomial expansions. Concretely, we rely on the classical methodology of approximating the true, but complicated, underlying density f, via a simpler reference density ϕ, as follows

$$f(x) \approx f_N(x) = \phi(x) \sum_{n=0}^{N} c_n p_n(x),$$

where $(p_n)_{n=0}^N$ are polynomials that are orthogonal in a suitable norm. Option prices are then obtained by integrating the payoff function $H(x)$ against the pseudo-density $f_N(x)$, i.e.

$$\int H(x) f(x)\,\mathrm{d}x \approx \int H(x) f_N(x)\,\mathrm{d}x. \tag{1}$$

Orthogonal polynomial expansions have a long history and have been utilized for option pricing by several authors. Edgeworth type price expansions based on the Gaussian reference have been proposed in Jarrow and Rudd (1982), Madan and Milne (1994), and Ribeiro and Poulsen (2013), while Filipović *et al.* (2013), Barletta and Nicolato (2018), and Asmussen and Bladt (2022) propose references based on the bilateral gamma, generalized inverse Gaussian, and normal inverse Gaussian distributions. In the pursuit of even more flexible reference densities, Ackerer and Filipović (2020) propose modeling ϕ as a mixture of Gaussian or gamma distributions. Lastly, we mention the work of Willems (2019), who considers expansions for Asian option prices in the Black-Scholes model based on a log-normal reference density. Common to all of these different contributions is the fact that the reference density is chosen to have a relatively simple analytic expression in order to allow for fast—if not explicit—computation of the pseudo-prices (1) for any order N. However, we observe that such computations may be carried out efficiently also without the explicit knowledge of ϕ. The key observation is to rewrite (1) as follows

$$\int H(x) f(x)\,\mathrm{d}x \approx \int H_N(x) \phi(x)\,\mathrm{d}x,$$

and interpret the pseudo-prices as integrals of the *polynomially scaled payoffs*

$$H_N(x) = H(x)\sum_{n=0}^{N} c_n p_n(x),$$

against the reference density ϕ. Therefore, we may select ϕ with explicit and tractable Laplace transform and efficiently evaluate the pseudo-prices via transform inversion methods. In this way, we circumvent any need for the explicit form of ϕ, thereby significantly broadening the scope of feasible references densities. The selection of ϕ is indeed crucial to attain good accuracy of the expansions already at low orders and avoid the well-known numerical issues occurring in the computation of the polynomial coefficients c_n at high orders. In this work, we utilize this combination of the classical orthogonal polynomial expansions approach with Fourier transform methods to approximate SVJJ-G prices. Based on the structural similarities between the SVJJ-E and the SVJJ-G models, we use the unknown density of the SVJJ-E specification as a reference and exploit the tractability of the SVJJ-E Laplace transform to construct low order, accurate, and fast approximations to the true SVJJ-G option prices. In particular, we re-conduct the joint calibration experiments performed for the SVJJ-G model to obtain essentially identical results, but using only a fraction of the computational time employed by exact transform based pricing.

The rest of the paper is structured as follows. In Section 2 we provide a summary of the SVJJ modeling framework, along with the necessary tools required for the joint calibration. We then present the model specifications to be tested and perform several calibrations of these. Section 3 gives a brief outline of the general theory of option pricing via orthogonal density expansions and derives the modified methodology that will be used to construct the pricing approximations. In Section 4 we specify the exact approximation scheme and perform some robustness checks along with a full joint calibration using the approximations. Section 5 concludes.

2. Testing alternative jump specifications for the SVJJ model

We assume that the SPX index follows the SVJJ model of Duffie *et al.* (2000), an affine stochastic volatility model where both the price and its variance display jumps. After a recap of the general SVJJ model characteristics, we consider a selection of concrete specifications and we compare their performances in a series of joint calibrations to SPX and VIX option data.

2.1. *Essentials of the SVJJ model*

We consider a normalized economy with zero interest rates and dividend yields, and we model the risk—neutral dynamics of the SPX log-price process X and its instantaneous variance V as follows

$$\mathrm{d}X_t = -\left(\bar{\mu} + \frac{1}{2}V_t\right)\mathrm{d}t + \sqrt{V_t}\,\mathrm{d}W_t^X + \mathrm{d}Z_t^X,$$

$$\mathrm{d}V_t = \kappa\,(\bar{v} - V_t)\,\mathrm{d}t + \varepsilon\sqrt{V_t}\,\mathrm{d}W_t^V + \mathrm{d}Z_t^V, \tag{2}$$

where $\bar{\mu} \in \mathbb{R}$, κ, $\bar{v}$ and ε are positive, $W = (W^X, W^V)$ is a Brownian motion and $Z = (Z^X, Z^V)$ is a compound Poisson process taking values in $\mathbb{R} \times \mathbb{R}_+$, independent of W. We assume that the correlation ρ between W^X and W^V is non-positive, as this is typically the case in equity markets. Regarding the process Z, let $\lambda > 0$ denote the intensity parameter and let $\mathcal{L}_J$ denote the Laplace transform of the jump size $J = (J^X, J^V)$, i.e.

$$\mathcal{L}_J(u, w) = \mathbb{E}\left[e^{uJ_X + wJ_V}\right], \tag{3}$$

defined for arguments in the domain $\mathcal{D}_J = \{(u, w) \in \mathbb{C}^2 : \mathbb{E}[|e^{uJ_X+wJ_V}|] < \infty\}$. At this stage, we do not specify further the distribution of J. We only require that the point $(1, 0)$ lays in $\mathcal{D}_J$ and we set $\bar{\mu} = \lambda(\mathcal{L}_J(1, 0) - 1)$ to ensure that the price process $S = e^X$ is a well defined martingale.

Duffie *et al.* (2000) show that the Laplace transform of the log-price X_T takes the form

$$\mathcal{L}_{X_T}(u) = \mathbb{E}\left[e^{uX_T}\right] = e^{uX_0 + A_X(T,u) + B_X(T,u)V_0 + C_X(T,u)},$$

where the functions A_X, B_X and C_X are given by

$$\begin{aligned}
A_X(T,u) &= -\kappa\bar{v}\left(\frac{\gamma+\beta}{\varepsilon^2}T\right.\\
&\qquad \left. + \frac{2}{\varepsilon^2}\log\left(1 - \frac{\gamma+\beta}{2\gamma}(1 - e^{-\gamma T})\right)\right)\\
B_X(T,u) &= -\frac{\alpha(1 - e^{-\gamma T})}{2\gamma - (\gamma+\beta)(1 - e^{-\gamma T})}\\
C_X(T,u) &= -(\lambda + \bar{\mu}\,u)T + \lambda\int_0^T \mathcal{L}_J(u, B_X(s,u))\,\mathrm{d}s,
\end{aligned} \tag{4}$$

with $\mathcal{L}_J$ defined in (3) and

$$\begin{aligned}
\alpha &= u(1-u), \quad \beta = u\rho\varepsilon - \kappa,\\
\gamma &= \sqrt{(\kappa - u\rho\varepsilon)^2 - \varepsilon^2(u^2 - u)}.
\end{aligned} \tag{5}$$

With the transform $\mathcal{L}_{X_T}$ at hand, we may price European-style claims contingent on the SPX index by means of Fourier inversion techniques. In this work, we rely on the so-called Lewis approach outlined e.g. in Schmelzle (2010). For ease of reference, we recall the key pricing formula in the lemma below.

LEMMA 2.1 *Let Z be a real-valued random variable—the underlying asset—with Laplace transform $\mathcal{L}_Z(u) = \mathbb{E}[e^{uZ}]$ defined on $\mathcal{D}_Z = \{u \in \mathbb{C} : \mathbb{E}[|e^{uZ}|] < \infty\}$. Let H be a real-valued function—the payoff—such that $\mathbb{E}[H(Z)] < \infty$ and let $\mathcal{L}_H(u) = \int H(x)e^{ux}\,\mathrm{d}x$ denote its Laplace transform defined on $\mathcal{D}_H = \{u \in \mathbb{C} : \int |H(x)e^{ux}|\,\mathrm{d}x < \infty\}$. Assume there exists a real number u_r such that $u_r \in \mathcal{D}_H$, $-u_r \in \mathcal{D}_Z$ and either*

$$\int_{u_r - \mathrm{i}\infty}^{u_r + \mathrm{i}\infty} |\mathcal{L}_Z(-u)|\,\mathrm{d}u < \infty,$$

or

$$\int_{u_r - \mathrm{i}\infty}^{u_r + \mathrm{i}\infty} |\mathcal{L}_H(u)|\,\mathrm{d}u < \infty, \tag{6}$$

holds true. Then we may express $\mathbb{E}[H(Z)]$*—the claim's price—as follows*

$$\mathbb{E}\left[H(Z)\right] = \frac{1}{\mathrm{i}2\pi}\int_{u_r-\mathrm{i}\infty}^{u_r+\mathrm{i}\infty} \mathcal{L}_Z(-u)\mathcal{L}_H(u)\,\mathrm{d}u. \tag{7}$$

For call options on the SPX index, one typically uses the decomposition

$$\mathbb{E}\left[\max(e^{X_T}-K,0)\right] = S_0 - \mathbb{E}\left[\min(e^{X_T},K)\right],$$

and applies Lemma 2.1 to price the covered-call payoff $H(x)=\min(e^x,K)$. In this case, the transform $\mathcal{L}_H$ is given by

$$\mathcal{L}_H(u) = -\frac{K^{u+1}}{u^2+u}, \tag{8}$$

and it fulfills (6) for any $u_r \in \mathcal{D}_H = \{u\in\mathbb{C} : -1 < \Re(u) < 0\}$. The martingale property of the price process $S=e^X$ implies that the log-price transform $\mathcal{L}_{X_T}(u)$ is finite for $0 < \Re(u) < 1$. Thus, the covered-call can be evaluated according to (7), e.g. by setting $u_r = -1/2$.

We may use the same approach also to price options written on the CBOE VIX index as the underlying. Following the CBOE (2023) white paper, the VIX squared (VIX^2) tracks the price of a portfolio of SPX options which, up to strike-discretization error, statically replicates the value of a log-contract expiring 30 days ahead. Maintaining the simplification of zero interest rates and dividend yields, the VIX^2 at time T is then defined as follows

$$\mathrm{VIX}_T^2 = -\frac{2}{\tau}\mathbb{E}_T\left[(\log S_{T+\tau} - \log S_T)\right] \tag{9}$$

where $\tau = \frac{30}{365}$, S is the value of the SPX and the conditional expectation $\mathbb{E}_T$ is taken under the pricing risk-neutral measure. As first observed by Neuberger (1994), the value of the log-contract is closely related to the fair price of future realized variance. More precisely, let $RV_T^{T+\tau}$ denote the continuously sampled realized variance over the time interval $[T, T+\tau]$, i.e.

$$RV_T^{T+\tau} = \frac{1}{\tau}\lim_{\Delta\to 0}\sum_{n=1}^{N}(\log S_{t_n} - \log S_{t_{n-1}})^2, \tag{10}$$

where $T = t_0 < t_1 < \ldots < t_N = T+\tau$ is an equally spaced partition of $[T, T+\tau]$ with step size $\Delta = \tau/N$. If the underlying SPX evolves according to a continuous semimartingale, it holds that

$$\mathbb{E}_T[RV_T^{t+\tau}] = -\frac{2}{\tau}\mathbb{E}_T\left[(\log S_{T+\tau} - \log S_T)\right], \tag{11}$$

and therefore the VIX^2 can be seen as a model-free risk-neutral estimate of the 30-days ahead realized variance. However, if the assumption of continuous dynamics is relaxed the relation (11) is only approximate due to an error induced by jumps in the return process. The mismatch between the log-contract premium—hence the VIX^2—and the variance swap rate under general discontinuous dynamics is carefully discussed in Broadie and Jain (2008) and Cont and Kokholm (2013), Section 4. Applying the results therein to the SVJJ model (2) we obtain that the approximation error in (11) is quantified by

$$\begin{aligned}\mathrm{VIX}_T^2 - \mathbb{E}_T[RV_T^{T+\tau}] &= 2\int_{\mathbb{R}}\left(e^{\xi} - 1 - \xi - \frac{\xi^2}{2}\right)\nu^X(\mathrm{d}\xi)\\ &= 2(\bar{\mu} - \mathbb{E}[Z_1^X]) - \mathrm{Var}[Z_1^X],\end{aligned}$$

where ν^X denotes the Lévy measure of Z^X. As for expression (9), a simple calculation shows that the VIX^2 is given by an affine transformation of the instantaneous variance

$$\mathrm{VIX}_T^2 = aV_T + b,$$

where

$$\begin{aligned}a &= \frac{1}{\kappa\tau}\left(1-e^{-\kappa\tau}\right),\\ b &= \frac{1}{\kappa}\left(\mathbb{E}\left[Z_1^V\right] + \kappa\theta\right)(1-a) + 2\left(\bar{\mu} - \mathbb{E}\left[Z_1^X\right]\right),\end{aligned} \tag{12}$$

so the Laplace transform of VIX_T^2 is given by

$$\mathcal{L}_{\mathrm{VIX}_T^2}(u) = e^{bu}\mathcal{L}_{V_T}(au),$$

where $\mathcal{L}_{V_T}$ is the Laplace transform of the instantaneous variance V_T. Following Sepp (2008) and Lian and Zhu (2013), $\mathcal{L}_{V_T}$ is given by

$$\mathcal{L}_{V_T}(u) = e^{A_V(T,u)+B_V(T,u)V_0+C_V(T,u)},$$

where the functions A_V, B_V and C_V read as follows

$$\begin{aligned}A_V(T,u) &= -\frac{2\kappa\bar{v}}{\varepsilon^2}\log\left(1+\frac{\varepsilon^2 u}{2\kappa}\left(e^{-\kappa T}-1\right)\right),\\ B_V(T,u) &= \frac{2\kappa u}{\varepsilon^2 u + \left(2\kappa - \varepsilon^2 u\right)e^{\kappa T}},\\ C_V(T,u) &= \lambda\int_0^T \mathcal{L}_J(0, B_V(s,u))\,\mathrm{d}s - \lambda T,\end{aligned} \tag{13}$$

with $\mathcal{L}_J$ defined in (3). A VIX call option, seen as a contract written on the VIX^2, has payoff function $H(x)=\max(\sqrt{x}-K,0)$ with transform $\mathcal{L}_H$ given by

$$\mathcal{L}_H(u) = \left(\frac{1}{-u}\right)^{\frac{3}{2}}\frac{\sqrt{\pi}}{2}\left(1-\mathrm{erf}\left(K\sqrt{-u}\right)\right), \tag{14}$$

where $\mathrm{erf}(z) = \frac{2}{\sqrt{\pi}}\int_0^z e^{-s^2}\,\mathrm{d}s$ is the complex-valued error function, and $u\in\mathcal{D}_H = \{u\in\mathbb{C} : \Re(u) < 0\}$. Since the integrability condition (6) is fulfilled for any $u_r < 0$, we may compute VIX calls and futures prices via (7) whenever 0 belongs to the interior domain of the transform $\mathcal{L}_{\mathrm{VIX}_T^2}$.

2.2. *A selection of jump specifications*

To complete the description of the model dynamics (2), one needs to specify the distribution of the jump-size $J = (J^X, J^V)$. Most applications keep to the original suggestion

of Duffie *et al.* (2000) and model the jump in variance J^V by an exponential law with mean value $1/\eta$, i.e. with Laplace transform $\mathcal{L}_{J^V}(w) = \mathcal{L}_J(0, w)$ given by

$$\mathcal{L}_{J^V}(w) = \frac{\eta}{\eta - w}, \quad \text{for } \Re(w) < \eta. \tag{15}$$

As for the jump in log-price J^X, it is modeled as follows

$$J^X = \mathcal{N}(\mu_x, \sigma_x^2) + \rho_J J^V, \tag{16}$$

where $N(\mu_x, \sigma_x^2)$ is a normal distribution with mean μ_x and variance σ_x^2 which is independent of J^V. The parameter $\rho_J \in \mathbb{R}$ regulates the correlation between jumps in log-price and jumps in variance. The joint jump transform $\mathcal{L}_J$ is then given by

$$\mathcal{L}_J(u, w) = \exp\left(u\mu_x + u^2\frac{\sigma_x^2}{2}\right)\mathcal{L}_{J^V}(u\rho_J + w), \tag{17}$$

with $\mathcal{L}_{J^V}$ specified in (15). An attractive feature of this specification, which we will refer to as the SVJJ-E model, is that both $\mathcal{L}_X$ and $\mathcal{L}_V$ are computable in terms of elementary functions. Specifically, the function C_X in (4) reads as follows

$$C_X(t, u) = -\lambda(1 + \bar{\mu}\, u)t + \lambda \exp\left(u\mu_x + u^2\frac{\sigma_x^2}{2}\right) D_X(t, u)$$

where $D_X(t, u)$ is given by

$$D_X(t, u) = \frac{(\gamma - \beta)t}{(\gamma - \beta)\delta + \alpha/\eta} - \frac{2\alpha/\eta}{(\gamma\delta)^2 - (\beta\delta - \alpha/\eta)^2} \log\left\{1 - \frac{(\gamma + \beta)\delta - \alpha/\eta}{2\gamma\delta}\left(1 - e^{-\gamma t}\right)\right\},$$

with α, β and γ as in (5) and $\delta = (1 - \rho_J u/\eta)$. As for the function C_V in (13), it is given by

$$C_V(t, u) = \begin{cases} \lambda\dfrac{2}{2\kappa - \varepsilon^2\eta} \log\left(1 + \frac{(2\kappa - \varepsilon^2\eta)u}{2\kappa(\eta - u)}\left(1 - e^{-\kappa t}\right)\right) & \text{if } 2\kappa - \varepsilon^2\eta \neq 0, \\ \lambda\dfrac{u}{\kappa(\eta - u)}\left(1 - e^{-\kappa t}\right) & \text{if } 2\kappa - \varepsilon^2\eta = 0. \end{cases}$$

Thus, under the SVJJ-E dynamics we can price SPX and VIX options very efficiently by numerically integrating (7) as the integrands involve only elementary functions. The study by Kokholm and Stisen (2015), however, indicates that the SVJJ-E does not provide satisfactory fits when jointly calibrated to SPX and VIX option data. Furthermore, Nicolato *et al.* (2017) suggest that modeling the jump in variance J^V with other distributions than the exponential one may lead to implied volatility curves which better resemble those empirically observed. Therefore we propose to maintain the structure (16) for the log-price jump J^X, but we consider two alternative specifications for the law of J^V: The SVJJ-G model where the jumps in variance are distributed according to a gamma law with Laplace transform

$$\mathcal{L}_{J^V}(w) = \left(\frac{\eta}{\eta - w}\right)^\theta, \quad \text{for } \Re(w) < \eta, \tag{18}$$

and the SVJJ-IG model where the jumps in variance are distributed according to an inverse Gaussian law with

$$\mathcal{L}_{J^V}(w) = \exp\left(\frac{\eta}{\theta}\left(1 - \sqrt{1 - \frac{2\theta^2 w}{\eta}}\right)\right) \quad \text{for } \Re(w) < \frac{\eta}{2\theta^2}.$$

In both cases, the joint jump transform $\mathcal{L}_J$ is still given by (17), albeit with the suitable choice for $\mathcal{L}_{J^V}$. Unfortunately, neither of these specifications allows for computing the functions C_X and C_V in closed form, meaning that an extra numerical integration is needed to evaluate $\mathcal{L}_X$ and $\mathcal{L}_V$ at each point. As we shall see, this significantly slows down the computation of option prices via the transform inversion (7).

2.3. Joint calibration to SPX and VIX options

We are now all set to run a horse-race between the SVJJ-E, SVJJ-G and SVJJ-IG models and asses their capability to fit SPX and VIX option data jointly. Given that the VIX futures prices are model dependent, these are also included in the calibration. For the task, we have obtained daily quotes on SPX/VIX options and VIX futures from OptionMetrics. We consider three periods of six weeks in each of the years 2018, 2019, and 2020 centered around the mid-dates 21/03/2018, 07/01/2019, and 22/05/2020. The last calibration period covers the COVID-19 lockdown and thus represents distressed market conditions. For all dates we filter out option quotes with zero bid price, options where the implied volatility cannot be computed, and in-the-money SPX options. For both SPX and VIX options, we consider maturities ranging from 1 week up to 18 months, when available. For SPX options, we choose an expanding window of moneyness which reflects the domain of liquidity for the various maturities. The precise intervals of log-moneyness $\log(K/S_0)$—where K is the option strike and S_0 is the spot SPX—corresponding to different maturities T are displayed in table 1. Given the mean-reverting nature of the VIX index, we do not impose any restriction on the moneyness of VIX options. However, we only consider VIX options for which a VIX futures with matching expiry is quoted. A common discount curve and the continuously compounded SPX dividend yield are backed out from near at-the-money calls and puts using the put-call parity. Finally, all quotes are filtered according to the no-arbitrage conditions of Carr and Madan (2005) such that there are no static arbitrage opportunities in the final option price data. This leaves us with an average of 301 SPX options and 84 VIX options on each date of our sample.

We carry out daily calibrations by minimizing weighted sums of mean-squared errors according to a modification of the objective function proposed in Kokholm and Stisen (2015)

Table 1. SPX log-moneyness $\log(K/S_0)$ intervals across maturities T.

Maturity	log-moneyness
$T < 2$ weeks	$[-0.2, 0.1]$
$T < 1$ month	$[-0.3, 0.15]$
$T < 6$ months	$[-0.7, 0.3]$
$T > 6$ months	$[-1, 0.5]$

to calibrate the standard SVJJ-E model. Specifically, we choose the following objective function

$$
\begin{aligned}
L(\Theta) = & \\
& \frac{1}{\#\text{SPX}} \sum_{T \in \mathcal{T}^{\text{SPX}}} \sum_{K \in \mathcal{K}_T^{\text{SPX}}} \\
& \quad \times \left(\frac{C_{\text{SPX}}^{\text{model}}(T,K;\,\Theta) - C_{\text{SPX}}^{\text{market}}(T,K;\,\Theta)}{C_{\text{SPX}}^{\text{market}}(T,K;\,\Theta)} \right)^2 \\
& + \frac{1}{\#\text{VIX}} \sum_{T \in \mathcal{T}^{\text{VIX}}} \sum_{K \in \mathcal{K}_T^{\text{VIX}}} \\
& \quad \times \left(\frac{C_{\text{VIX}}^{\text{model}}(T,K;\,\Theta) - C_{\text{VIX}}^{\text{market}}(T,K;\,\Theta)}{C_{\text{VIX}}^{\text{market}}(T,K;\,\Theta)} \right)^2 \\
& + \frac{\mathcal{W}}{\#\text{VIX}} \sum_{T \in \mathcal{T}^{\text{FUTURES}}} \left(\frac{F_{\text{VIX}}^{\text{model}}(T;\,\Theta) - F_{\text{VIX}}^{\text{market}}(T;\,\Theta)}{F_{\text{VIX}}^{\text{market}}(T;\,\Theta)} \right)^2 .
\end{aligned} \tag{19}
$$

where Θ denotes the set of model parameters, $\mathcal{T}$ the set of maturities and $\mathcal{K}_T$ the set of strikes associated with maturity $T \in \mathcal{T}$. #VIX denotes the number of VIX products, i.e. the sum of both VIX options and futures. $\mathcal{W}$ weighs the impact of VIX futures on $L(\Theta)$, and by setting $\mathcal{W} = 1$ we recover the objective function of Kokholm and Stisen (2015). However, there are only about 8 VIX futures quotes per day against a 10 times larger number of VIX options. Matching the term structure of VIX futures as close as possible is indeed essential for the VIX implied volatilities to be meaningful. Therefore, we follow the suggestion of Guyon and Mustapha (2023) and we overweight the VIX futures of a factor $\mathcal{W} = 10$ to reflect the ratio between the number of VIX futures and options.

Option prices and futures are computed via transform inversion as explained in Section 2.1. The calibrations are performed using a gradient based optimization algorithm. Varying starting points for the optimization have been tried, but it seems that for reasonable initial guesses the same solution is obtained. Option implied volatilities are then obtained by inverting the Black-76 formula

$$
\begin{aligned}
C(T,K) = & F\Phi\left(\frac{\log(F/K)}{\sigma_{IV}(T,K)\sqrt{T}} + \frac{\sigma_{IV}(T,K)\sqrt{T}}{2} \right) \\
& - e^{-rT} K \Phi\left(\frac{\log(F/K)}{\sigma_{IV}(T,K)\sqrt{T}} - \frac{\sigma_{IV}(T,K)\sqrt{T}}{2} \right),
\end{aligned} \tag{20}
$$

where Φ denotes the cumulative distribution function of the standard normal distribution and F denotes the SPX or VIX futures price. We stress that for the fitted VIX prices, F is the model futures price.

We start by examining the calibration results of the alternative model specifications on the mid-dates of the three periods under consideration. Table 2 shows the calibrated parameters while table 3 reports the calibration errors separately for SPX options, VIX options and VIX futures. Figure 1 plots the observed and fitted implied volatilities on 07/01/2019. Similar plots for the remaining two dates are reported in figures A1 and A2 in Appendix 3.

We see that, on the selected dates, the SVJJ-G is clearly the best performing model with sizeable error reductions compared to both the standard SVJJ-E model and the SVJJ-IG model. Notably, most of the improvement comes from the fit to VIX options and futures.

However, figure 1 highlights that none of the model specifications provides fits which are fully satisfactory. While both the SVJJ-G and SVJJ-E models are capable to reproduce quite closely SPX implied volatilities for most maturities, none of the specifications can suitably fit VIX options with short maturities and low strikes. Figures A1 and A2 reveal similar results for the remaining mid-dates, indicating that the SVJJ *dynamics* are too simple to jointly capture the features of both SPX and VIX option markets.

Still, the improvement achieved solely by changing the variance jump distribution is remarkable and it is confirmed throughout the entire sample period. Figure 2 shows the

Table 2. Calibrated parameters for the three SVJJ model specifications.

Model	κ	$\bar{v}$	ε	λ	θ	η	μ_X	σ_X	ρ	ρ_J
SVJJ-E										
21/03/2018	1.14	0.007	0.69	0.072		2.00	−0.06	0.16	−0.64	−0.40
07/01/2019	0.96	0.003	0.49	0.057		3.03	−0.32	0.36	−0.68	−0.15
22/05/2020	1.34	0.073	1.14	0.15		1.41	0.02	0.14	−0.68	−0.48
SVJJ-G										
21/03/2018	4.99	0.020	0.80	0.106	1.80	1.31	0.01	0.12	−0.64	−0.28
07/01/2019	5.27	0.033	0.72	0.047	0.34	0.45	−0.04	0.16	−0.68	−0.28
22/05/2020	4.50	0.084	1.58	0.12	1.64	1.24	0.09	0.13	−0.78	−0.22
SVJJ-IG										
21/03/2018	2.06	0.025	0.70	0.046	0.90	6.94	0.03	0.42	−0.65	−0.21
07/01/2019	3.45	0.026	0.62	0.046	0.58	4.97	−0.02	0.32	−0.75	−0.17
22/05/2020	2.26	0.090	1.43	0.041	2.05	3.96	0.02	0.20	−0.44	−0.33

Table 3. Average relative errors of SPX and VIX option implied volatilities as well as VIX futures prices across the three calibrated SVJJ model specifications on the three separate dates 21/03/2018, 07/01/2019, and 22/05/2020.

Model	SPX	VIX	VIX futures
		SVJJ-E	
21/03/2018	2.07% (0.0167)	28.1% (0.2191)	19.59% (0.0402)
07/01/2019	1.05% (0.0054)	15.44% (0.1058)	4.26% (0.0018)
22/05/2020	2.66% (0.0408)	9.93% (0.0688)	3.58% (0.0015)
		SVJJ-G	
21/03/2018	1.71% (0.0026)	11.50% (0.0878)	1.23% (0.0002)
07/01/2019	0.96% (0.0027)	12.23% (0.1073)	3.05% (0.0010)
22/05/2020	2.63% (0.0297)	7.72% (0.0463)	3.41% (0.0014)
		SVJJ-IG	
21/03/2018	4.47% (0.0162)	18.31% (0.1131)	2.97% (0.0011)
07/01/2019	2.26% (0.0122)	25.78% (0.1312)	7.04% (0.0051)
22/05/2020	3.10% (0.0415)	18.28% (0.0566)	8.08% (0.0072)

Note: Mean squared pricing errors are shown in parentheses.

results of the calibrations for each of the model specifications over the three time intervals under consideration. For ease of interpretation, we report separately the 3-days moving average of the daily average relative errors of SPX implied volatilities (top panel), VIX implied volatilities (mid panel) and VIX futures (bottom panel). The summary statistics for the full sample are reported in table 4.

The SVJJ-G models consistently outperforms both the standard SVJJ-E model and the SVJJ-IG model which, all in all, is the clear loser of the calibration race. Even if for a few days in 2018 the SVJJ-IG fits to VIX implied volatilities and futures are superior to those of the SVJJ-G specification, the corresponding fits to SPX implied volatilities are categorically worse.

Considering the SPX errors in isolation, we once again notice that the improvements of the SVJJ-G model over the SVJJ-E model, although consistent, are somewhat limited. However, when looking at VIX errors we clearly see the impact of the alternative jump distributions. Table 4 shows that the SVJJ-G calibration errors to VIX implied volatilities are on average ca. 20% lower than in the SVJJ-E case and 40% lower than in the SVJJ-IG case. Similarly, for VIX futures, the SVJJ-G errors are on average ca. 30% and 40% lower than in the SVJJ-E and SVJJ-IG case.

In conclusion, our analysis shows that simply by exploring alternative jump distributions, one may substantially improve the performance of the joint calibration in a parsimonious way. One possible drawback is that selecting more flexible but less tractable distributions might result in an increased computational burden. This is exactly the case for the SVJJ-G model. Table 5 reports the average daily calibration times for the SVJJ-G, SVJJ-E and SVJJ-IG specifications.

Pricing under the SVJJ-G dynamics entails an extra numeric integration to compute the transform (17), heavily affecting the transform inversion (7) both for SPX and VIX options. The calibration time for the SVJJ-G model is about 10 times longer than for the standard SVJJ-E, tainting the comparatively superior model fits. In the following sections we therefore seek to facilitate the computational aspect by means of constructing efficient and accurate option price approximations.

3. Polynomial price expansions by transform inversion

In this section we first recap the methodology of approximating an unknown density f in terms of a simpler density ϕ and its associated orthonormal polynomials. For a detailed exposition we refer e.g. to Szegö (1939). Next, we show how to combine the density expansions approach with transform inversion methods to price options accurately and efficiently.

3.1. *Density expansions—a brief recap*

Let Z be a random variable with density function f—the *target*—which is unknown, and let H be a sufficiently integrable function so that the expectation

$$\mathbb{E}[H(Z)] = \int H(x)f(x)\,\mathrm{d}x, \tag{21}$$

is finite. In the context of this work, we think of Z as the risk-neutral distribution of the SPX log-price X_T or the distribution of the VIX_T^2, while H represents either the SPX covered-call payoff or the VIX call payoff introduced in Section 2.1. Our goal is to expand the target f in a sequence of functions $(f_N)_{N\in\mathbb{N}}$ such that

(i) The approximating functions, termed the *pseudo-densities*, converge to the target density

$$\|f - f_N\| \to 0 \quad \text{as } N \to \infty, \tag{22}$$

where $\|\cdot\|$ is a suitable norm to be defined below.

(ii) The corresponding approximate prices, termed the *pseudo-prices*, are computable in closed form and converge to the true price

$$\int H_N(x)f(x)\,\mathrm{d}x \to \int H(x)f(x)\,\mathrm{d}x \quad \text{as } N \to \infty. \tag{23}$$

We follow the classical methodology of approximating the target density f via a probability measure ν with density ϕ—here termed the *reference* measure and density—corrected

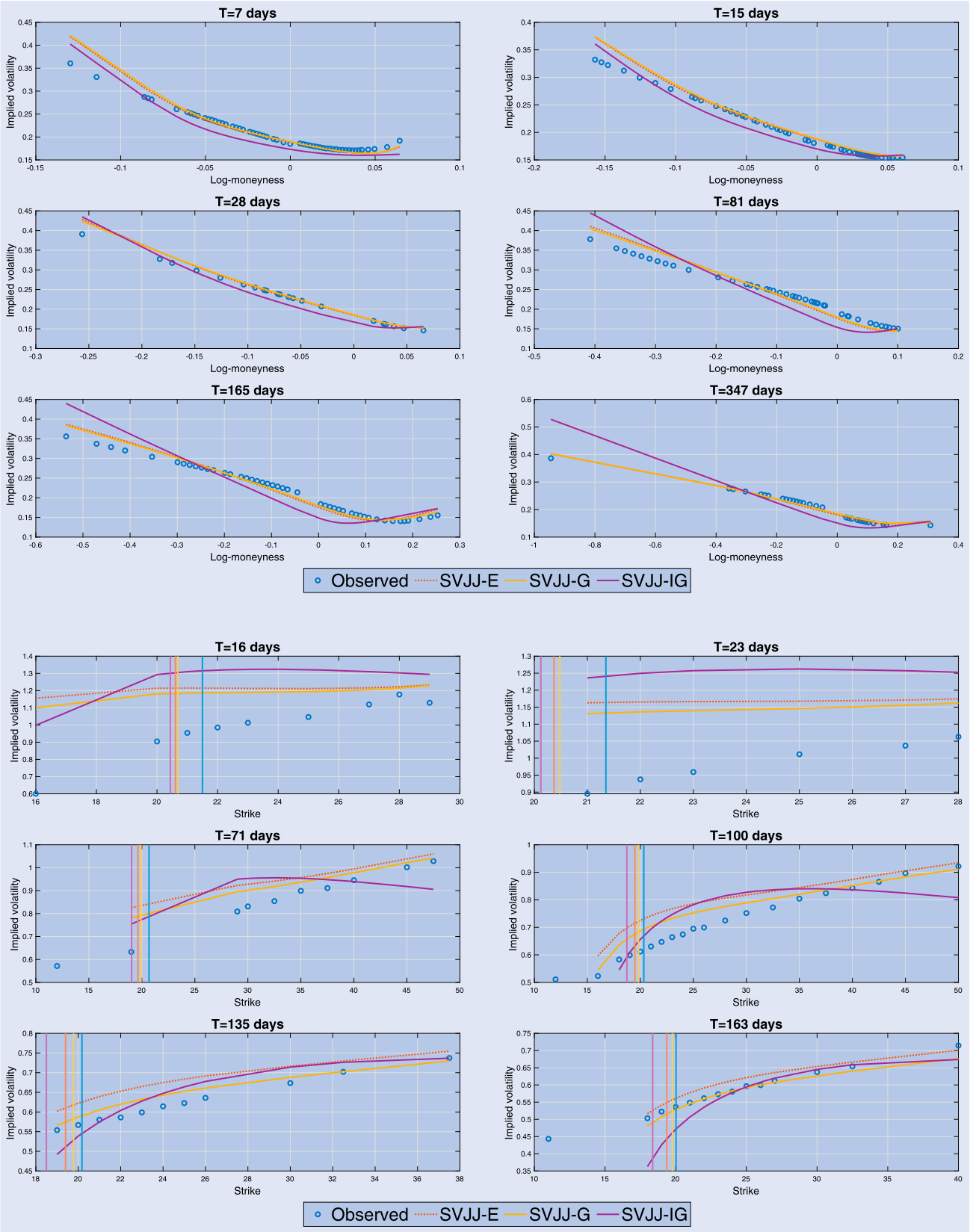

Figure 1. SPX and VIX implied volatility fits on January 7th 2019. VIX futures prices are represented by vertical lines. SPX implied volatilities are plotted against log-moneyness $\log(K/S_0)$.

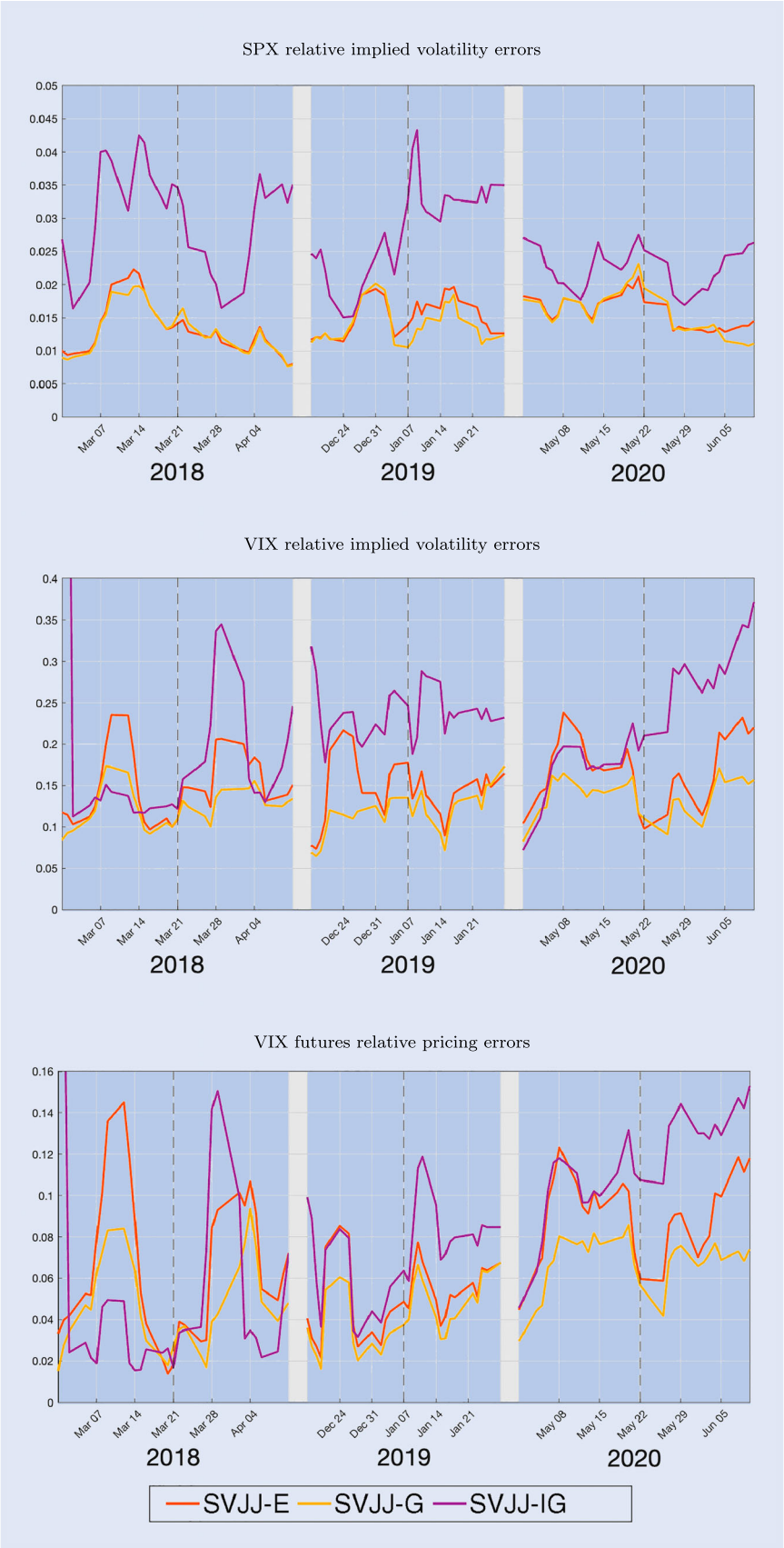

Figure 2. 3-day moving averages of the average relative errors of SPX and VIX implied volatilities, as well as VIX futures prices. Breaks between the three periods under consideration are represented by shaded regions and the dashed vertical lines indicate the middle sampling dates.

Table 4. Summary statistics of the implied volatility average relative errors over all the conducted calibrations.

Market	Mean	Std. Dev.	Min	Max
SPX				
SVJJ-E	0.0148	0.0043	0.0049	0.0277
SVJJ-G	0.0139	0.0042	0.0047	0.0263
SVJJ-IG	0.0272	0.0096	0.0107	0.0602
VIX				
SVJJ-E	0.1965	0.0707	0.0783	0.3564
SVJJ-G	0.1611	0.0577	0.0572	0.2958
SVJJ-IG	0.2726	0.2670	0.0996	0.5740
		VIX Futures		
SVJJ-E	0.0689	0.0401	0.0073	0.1730
SVJJ-G	0.0499	0.0316	0.0040	0.1574
SVJJ-IG	0.0830	0.0804	0.0038	0.4590

Table 5. Average daily calibration times for the three models in the three selected periods.

	2018	2019	2020
SVJJ-E	188 s	193 s	235 s
SVJJ-G	1495 s	1622 s	1506 s
SVJJ-IG	1897 s	1641 s	1606 s

with linear combinations of polynomials orthogonal with respect to the norm induced by the reference itself. The approach can be schematically outlined as follows.

Step 1. First select the reference probability measure ν with finite moments of all order, i.e.

$$\int |x^n| \nu(\mathrm{d}x) < \infty, \quad \text{for all } n = 1, 2, \ldots. \tag{24}$$

Then we can find a set of polynomials $(p_n)_{n\in\mathbb{N}_0}$ which are orthonormal in the space $L^2(\nu)$ equipped with the usual inner product $\langle f, g\rangle = \int fg \,\mathrm{d}\nu$ and the associated norm $\|g\|^2 = \langle g, g\rangle$. That is, the $(p_n)_{n\in\mathbb{N}_0}$ satisfy

$$\langle p_i, p_j\rangle = \int p_j(x)p_j(x)\nu(\mathrm{d}x) = \delta_{ij}, \quad i,j \in \mathbb{N}_0,$$

where δ_{ij} denotes the Kronecker symbol. Such polynomials can be constructed e.g. via the Gram-Schmidt orthogonalization procedure based on the three-term recurrence for orthogonal polynomials: Fixing the initial conditions

$$p_{-1}(x) \equiv 0, \quad p_0(x) \equiv 1,$$

for $n = 0, 1, 2, \ldots$, it holds that

$$p_{n+1}(x) = \frac{1}{\sqrt{\langle \pi_{n+1}, \pi_{n+1}\rangle}} \pi_{n+1}(x),$$

where

$$\pi_{n+1}(x) = (x - B_n)p_n(x) - C_n p_{n-1}(x),$$

and the coefficients B_n, C_n are given as

$$B_n = \langle xp_n, p_n\rangle, \quad C_n = \langle xp_n, p_{n-1}\rangle.$$

Notice that computing the relevant inner products requires the moments of the reference measure ν up to order $2N$ as well as the polynomial coefficients of previous orders. It is therefore important to choose a reference measure for which it is possible to efficiently compute moments of arbitrary order.

Although the Gram-Schmidt construction detailed above ensures that the polynomials $(p_n)_{n\in\mathbb{N}_0}$ form an orthogonal set, they do not necessarily form a complete set in $L^2(\nu)$. A sufficient condition for completeness is that

$$\exists\, \alpha > 0 \quad \text{such that} \int_{\mathbb{R}} e^{\alpha|x|} \nu(\mathrm{d}x) < \infty. \tag{25}$$

Step 2. Under the additional assumption that the likelihood ratio f/ϕ is in $L^2(\nu)$, we may proceed to expand f by projecting f/ϕ onto the $\mathrm{span}(p_n)_{n\in\mathbb{N}_0}$. More precisely, if the following holds

$$\int \frac{f^2(x)}{\phi^2(x)} \,\mathrm{d}\nu(x) = \int \frac{f^2(x)}{\phi(x)} \,\mathrm{d}x < \infty, \tag{26}$$

we obtain that

$$\frac{f(x)}{\phi(x)} = \sum_{n=0}^{\infty} c_n p_n(x),$$

where the coefficients c_n are given by

$$c_n = \langle f/\phi, p_n\rangle = \int p_n(x) f(x) \,\mathrm{d}x. \tag{27}$$

In other words, we may approximate the target f with the pseudo-densities

$$f(x) \approx f_N(x) = \phi(x) \sum_{n=0}^{N} c_n p_n(x), \tag{28}$$

and the desired convergence (22) is guaranteed.

Step 3. Finally, we may approximate the true price (21) with the pseudo-prices obtained from integrating the payoff function H against f_N, i.e.

$$\int H(x) f(x) \,\mathrm{d}x \approx \int H(x) f_N(x) \,\mathrm{d}x, \tag{29}$$

for a suitable order N. A simple application of the Cauchy-Schwartz inequality shows that, under the assumption (26), the convergence (23) of the pseudo-prices to the exact price is attained whenever the payoff H lies in $L^2(\nu)$, i.e.

$$\int H^2(x)\phi(x) \,\mathrm{d}x < \infty.$$

Thus, one may apply the outlined pricing approach to evaluate bounded payoffs (such as put options or the covered call contract) or payoffs with power growth (such as VIX options in the SVJJ framework).

We conclude this section with a couple of remarks concerning the convergence of the pseudo-densities f_N to the target f.

REMARK 1 First, we notice that the computation of the coefficients c_n in (27) only requires the moments of the target density f. Therefore, we may define the pseudo-densities f_N according to (28) and the corresponding pseudo-prices in (29) even if the convergence condition (26) is not verified, but the less restrictive condition

$$\int |x^n| f(x)\,\mathrm{d}x < \infty, \quad \text{for all } n = 1, 2, \ldots, \tag{30}$$

is fulfilled. Although such pseudo-densities and pseudo-prices do not necessarily converge to the exact quantities, they might still provide accurate approximations for f and $\mathbb{E}[H(Z)]$. See e.g. Ackerer and Filipović (2020) who discuss orthogonal polynomial expansions based on reference densities ϕ violating (26) to approximate option prices in continuous stochastic volatility models.

REMARK 2 Of the assumptions listed above, the convergence condition (26) is arguably the most difficult to check, as the target density f is not available explicitly. In fact, as we discuss in Section 3.2 below, even the reference ϕ might not be known in closed form. However, one may—at least heuristically—infer the asymptotic behavior of f and ϕ from the knowledge of their relevant critical moments.

To be more precise, consider first a target f with support on the entire real line $\mathbb{R}$, let u_f^+ and u_f^- denote its critical exponential moments, i.e.

$$u_f^+ = \sup\left\{u \in \mathbb{R} : \int_{\mathbb{R}} e^{ux} f(x)\,\mathrm{d}x < \infty\right\}, \tag{31}$$

$$u_f^- = \inf\left\{u \in \mathbb{R} : \int_{\mathbb{R}} e^{ux} f(x)\,\mathrm{d}x < \infty\right\}, \tag{32}$$

and assume that $u_f^+ > 0$, and $u_f^- < 0$, are both finite. Under sufficient regularity conditions, we may conclude that the tails of the density f decay exponentially with rates dictated by the critical exponential moments. That is,

$$f(x) = \begin{cases} e^{\left(-u_f^+ + o(1)\right)x}, & \text{as } x \to +\infty, \\ e^{\left(-u_f^- + o(1)\right)x}, & \text{as } x \to -\infty. \end{cases} \tag{33}$$

Similarly, consider a reference ϕ with finite critical exponential moments $u_\phi^+ > 0$, and $u_\phi^- < 0$, and assume that the tail behavior of ϕ is as in (33) albeit with u_ϕ^+ and u_ϕ^- as exponential rates. Then it is clear that the convergence condition (26) is satisfied whenever

$$u_\phi^+ < 2u_f^+ \quad \text{and} \quad u_\phi^- > 2u_f^-. \tag{34}$$

Consider now the case of a target f with support on the positive real line $\mathbb{R}_+$. Here we make the heuristic assumption that if f has finite critical upper exponential moment $u_f^+ > 0$ and finite critical *negative moment* $q_f^- < 0$, defined as

$$q_f^- = \inf\left\{q \in \mathbb{R} : \int_{\mathbb{R}_+} x^q f(x)\,\mathrm{d}x < \infty\right\}, \tag{35}$$

then the following holds

$$f(x) = \begin{cases} e^{\left(-u_f^+ + o(1)\right)x}, & \text{as } x \to +\infty, \\ x^{-q_f^- - 1 + o(1)}, & \text{as } x \to 0. \end{cases} \tag{36}$$

So, if we consider a reference ϕ with support on $\mathbb{R}_+$, with finite $u_\phi^+ > 0$ and $q_\phi^- < 0$ and once again we assume that ϕ behaves asymptotically as (36), we may conclude that the convergence condition (26) is satisfied whenever

$$u_\phi^+ < 2u_f^+ \quad \text{and} \quad q_\phi^- > 2q_f^-. \tag{37}$$

3.2. *Price expansions—revisited*

The choice of the reference density ϕ is a pivotal step of the polynomial expansion approach described above. It is well known that even if ϕ complies to condition (26), hereby guaranteeing the theoretical convergence of the pseudo-densities f_N to the target f, in practice we cannot take N arbitrarily large, due to numerical errors occurring when computing the coefficients c_n given in (27) at high orders. To illustrate this issue, we apply the methodology to approximate the log-price density in the Heston (1993) model, here denoted by $f_{X_T^0}$, and price a set of SPX put options according to (29). The dynamics of the log-price and variance pair (X^0, V^0) are obtained by switching off jumps in the general SVJJ framework, i.e. by setting $Z^X = Z^V = 0$ in (2). Following Filipović *et al.* (2013), we specify the reference measure as a variance gamma distribution with density given by

$$\phi_{VG}(x) = \frac{(\alpha^2 - \beta^2)^\lambda}{\sqrt{\pi}(2\alpha)^{\lambda - 1/2}\Gamma(\lambda)} e^{\beta(x-\mu)} |x - \mu|^{\lambda - 1/2} K_{\lambda - 1/2}(\alpha|x - \mu|), \quad x \in \mathbb{R} \tag{38}$$

where $\lambda > 0$, $0 \le |\beta| < \alpha$, $\mu \in \mathbb{R}$ and $K_\omega(x)$ is a modified Bessel function of the second kind. The corresponding Laplace transform reads as follows

$$\mathcal{L}_{VG}(u) = e^{\mu u}\left(\frac{\alpha^2 - \beta^2}{\alpha^2 - (\beta + u)^2}\right)^\lambda, \tag{39}$$

and it shows that ϕ_{VG} satisfies the completeness assumption (25). We fix the maturity at $T = 1$ and consider two sets of Heston parameters. In the base case we set $\kappa = 1.5$, $\bar{v} = 0.04$, $V_0^0 = 0.03$, $\rho = -0.75$ and $\varepsilon = 0.22$. In the second specification, we stress the vol-of-vol parameter to a higher value and set $\varepsilon = 0.8$. The variance gamma parameters $(\mu, \alpha, \beta, \lambda)$ are chosen so that the first four moments of the reference density ϕ_{VG} match those of the target log-price density $f_{X_T^0}$. In Appendix 1 we show that the resulting ϕ_{VG} fulfills the convergence condition (26) in both the low and the high vol-of-vol scenarios. The performances of the corresponding polynomial expansions, however, differ considerably. Figure 3 plots the exact Heston implied volatility curve and its approximations of order $N = 0,7,20$ over a log-moneyness interval $\log(K/S_0) \in [-30\% + 45\%]$. We see that in the low vol-of-vol case, the $N = 0$ order approximation—that is the reference ϕ_{VG} itself—is already capturing most of the exact curve, and

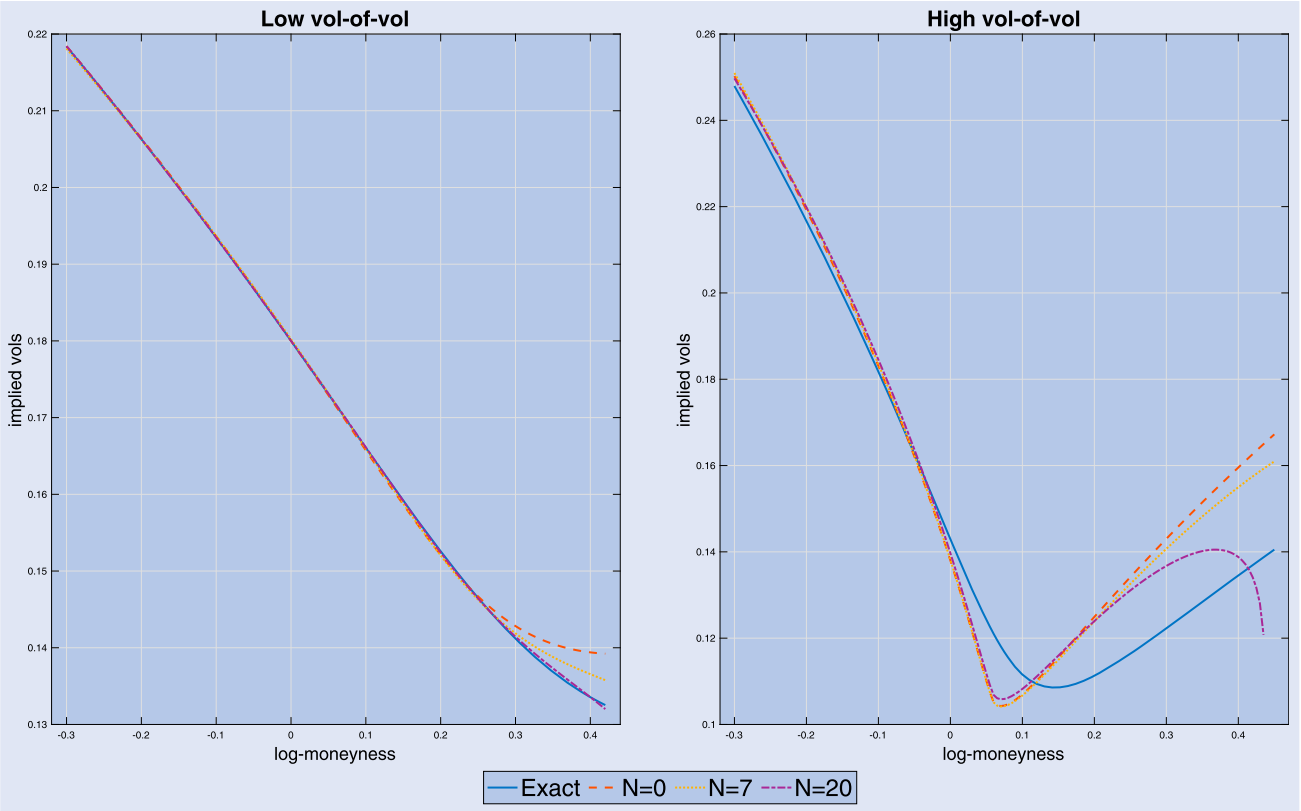

Figure 3. SPX implied volatilities in the Heston model under the low vol-of-vol (left panel) and the high vol-of-vol (right panel) scenarios. The curves correspond to orthogonal expansions based on the VG reference of order $N = 0,7,20$ benchmarked against the exact Heston implied volatilities.

the mismatch exhibited at large strikes essentially disappears when the order is increased to $N = 20$. Under the high vol-of-vol specification, by contrast, the reference density needs a substantial correction and the seemingly slow convergence appears to be hindered by numerical irregularities occurring already at $N = 20$.

It is therefore crucial to choose the reference measure as close as possible to the target to yield accurate approximations already at low orders N.

As already mentioned, a number of authors have proposed a variety of increasingly flexible distributions ν with explicitly computable density ϕ. This is an essential feature if one wishes to construct explicit pseudo-densities to approximate the target f. In this work, however, we are first and foremost concerned in approximating efficiently the exact option price via the pseudo-prices as in (29). To carry out such integrations fast and accurately, the explicit knowledge of the reference ϕ is not strictly required as long as the corresponding Laplace transform $\mathcal{L}_\nu(u) = \int e^{ux}\phi(x)\,\mathrm{d}x$ is available in closed form.

The key insight is simply to re-arrange the terms of the pseudo-price integrands as follows

$$\int H(x) f_N(x)\,\mathrm{d}x = \int H_N(x)\phi(x)\,\mathrm{d}x, \tag{40}$$

where H_N denotes the *polynomially scaled payoff*

$$H_N(x) = H(x)\sum_{k=0}^{N} c_k p_k(x). \tag{41}$$

We can then interpret the pseudo-prices as integrals of the polynomially scaled payoffs H_N against the reference density ϕ, rather than integrals of the payoff H against the pseudo densities f_N. Thus, if H_N admits a closed form Laplace transform

$$\mathcal{L}_{H_N}(u) = \int e^{ux} H_N(x)\,\mathrm{d}x,$$

we may evaluate the right hand side in (40) by transform inversion as described in Lemma 2.1.

Notice that if the option payoff H has a closed-form transform $\mathcal{L}_H$, then so does the polynomially scaled version H_N as $\mathcal{L}_{H_N}$ can be obtained via a simple differentiation of $\mathcal{L}_H$. More precisely, since $\mathcal{L}_H$ is analytic in its interior domain $\overset{\circ}{\mathcal{D}}_H$, its nth derivative $\mathcal{L}_H^{(n)} = \frac{\mathrm{d}^n}{\mathrm{d}u^n}\mathcal{L}_H$ is well defined and it is given by

$$\mathcal{L}_H^{(n)}(u) = \int e^{ux}\,(x^n H(x))\,\mathrm{d}x, \quad u \in \overset{\circ}{\mathcal{D}}_H,$$

implying that the transform $\mathcal{L}_{H_N}$ reads as follows

$$\mathcal{L}_{H_N}(u) = \sum_{n=0}^{N} q_n\,\mathcal{L}_H^{(n)}(u), \quad u \in \overset{\circ}{\mathcal{D}}_H, \tag{42}$$

where q_n, $n = 0, 1, \ldots, N$ are the coefficients such that

$$\sum_{n=0}^{N} q_n x^n = \sum_{k=0}^{N} c_k p_k(x).$$

To sum up, for a variety of common payoffs H, we may adopt the orthogonal polynomial approach to approximate the exact option price (21), but broadening the scope of potential reference measures ν to probability distributions that are only known up to their Laplace transform $\mathcal{L}_\nu$. In such a case, we simply add a final evaluation step to the procedure described in Section 3.1

Step 4. If the transforms $\mathcal{L}_\nu$ and $\mathcal{L}_H$ of the reference measure ν and payoff function H are known in closed form, compute the polynomially scaled payoff H_N and the corresponding transform $\mathcal{L}_{H_N}$ according to (41) and (42), respectively. If the assumptions of Lemma 2.1 are satisfied, approximate the exact option price as in (29) by computing the pseudo-price as follows

$$\int H(x) f_N(x)\,\mathrm{d}x = \frac{1}{\mathrm{i}2\pi}\int_{u_r-\mathrm{i}\infty}^{u_r+\mathrm{i}\infty} \mathcal{L}_\nu(-u)\mathcal{L}_{H_N}(u)\,\mathrm{d}u. \tag{43}$$

Remark 3 The transform-based evaluation of pseudo-prices offers a valuable alternative to the direct integration against pseudo-densities also for all those reference measures with explicit but complicated density ϕ and much simpler transform $\mathcal{L}_\nu$. The variance gamma distribution discussed above is a point in case: While the transform in (39) only contains elementary functions, the variance gamma density (38) involves the modified Bessel function and integrating against it may not be entirely free of complications.

Let us conclude by taking a closer look at the payoffs H relevant for this work, i.e. the SPX covered-call and the VIX call payoff discussed in Section 2. In both cases the transform derivatives $\mathcal{L}_H^{(n)}$—and thus the polynomially scaled transforms $\mathcal{L}_{H_N}$—allow for a closed-form expression which is easy to implement at any order.

For the SPX covered-call, rewrite (8) as follows

$$\mathcal{L}_H(u) = K^{u+1}\left(\frac{1}{u+1}-\frac{1}{u}\right), \quad -1<\Re(u)<0,$$

and apply the Leibniz rule to obtain

$$\mathcal{L}_H^{(n)}(u) = K^{u+1}\sum_{j=0}^{n}\binom{n}{j}(\log K)^{n-j}(-1)^j j!\left(\frac{1}{(u+1)^{j+1}}-\frac{1}{u^{j+1}}\right). \tag{44}$$

In particular, the polynomially scaled covered-call satisfies condition (6) for any $-1<u_r<0$, and we may apply the inversion (7) to compute pseudo-prices corresponding to any reference ν fulfilling the completeness assumption (25).

For the VIX call, we combine the fact that

$$\frac{\sqrt{\pi}}{2}\frac{\mathrm{d}}{\mathrm{d}u}\left(1-\operatorname{erf}\left(K\sqrt{-u}\right)\right) = \frac{K}{2}\frac{1}{(-u)^{\frac{1}{2}}}e^{K^2u},$$

and

$$\frac{\mathrm{d}^n}{\mathrm{d}u^n}\left(\frac{1}{(-u)^{m+\frac{1}{2}}}\right) = \frac{1}{(-u)^{m+n+\frac{1}{2}}}\frac{(2m+2n-1)!!}{2^n\,(2m-1)!!},$$

to obtain that the nth derivative of $\mathcal{L}_H$ given in (14) reads as follows

$$\mathcal{L}_H^{(n)}(u) = \frac{\sqrt{\pi}}{2}\frac{(2n+1)!!}{2^n}\frac{\left(1-\operatorname{erf}\left(K\sqrt{-u}\right)\right)}{(-u)^{n+\frac{3}{2}}} + Ke^{K^2u}\sum_{j=0}^{n-1}\frac{a_j}{(-u)^{2+j}}, \quad \Re(u)<0, \tag{45}$$

where

$$a_j = \frac{1}{2^j}\sum_{\ell=0}^{j}\binom{n}{\ell}\binom{n-\ell-1}{j-\ell}(2\ell+1)!!\,(2(j-\ell)-1)!!.$$

We see that $\mathcal{L}_{H_N}$ fulfills (6) for any $u_r<0$, and we may apply Lemma 2.1 to evaluate VIX call pseudo-prices for any choice of reference ν satisfying (25).

4. Polynomial price expansions in the SVJJ-G model

In this section we apply the orthogonal polynomials methodology to speed up the evaluation of SPX and VIX options in the SVJJ-G model, as we found it to be the best performing model specification in the calibrations performed in Section 2. We discuss the details of the approximations and the choice of the reference measure ν first for the underlying log-price X_T and then for the VIX_T^2. In both cases, the basic principle in choosing ν is to exploit the similarity of the SVJJ-G marginal distributions to those of simpler affine models with unknown densities but closed-form Laplace transform. We then assess the accuracy of the approximations with a series of calibrations both to model generated data as well as to the market data utilized in Section 2.

4.1. Approximating SPX option prices

The approximating methodology outlined in Section 3 requires that both the target distribution and the reference measure admit a density with respect to Lebesgue measure. Thus, our first task is to show that this is indeed the case for the marginal distributions of the SVJJ log-price process.

Proposition 4.1 *Consider the general SVJJ dynamics (2). Then, at any time $T>0$ the log-price distribution X_T is absolutely continuous with respect to the Lebesgue measure and its density function f_{X_T} is of class $\mathcal{C}^\infty$.*

Proof Fix $T>0$ and write the Laplace transform $\mathcal{L}_{X_T}$ of the T-time log-price X_T as follows

$$\mathcal{L}_{X_T}(u) = \mathcal{L}_{X_T^0}(u)\mathcal{L}_{X_T^J}(u), \tag{46}$$

where

$$\mathcal{L}_{X_T^0}(u) = e^{uX_0+A_X(T,u)+B_X(T,u)V_0} \quad \text{and} \quad \mathcal{L}_{X_T^J}(u) = e^{C_X(T,u)},$$

with A_X, B_X, C_X defined as in (4). Notice that $\mathcal{L}_{X_T^0}$ is the Laplace transform of the log-price X_T^0 in the Heston model.

More precisely $\mathcal{L}_{X_T^0} = \mathbb{E}[e^{X_T^0 u}]$ where the process X^0 has dynamics

$$\begin{aligned} \mathrm{d}X_t^0 &= -\frac{1}{2}V_t^0\,\mathrm{d}t + \sqrt{V_t^0}\,\mathrm{d}W_t^X, \\ \mathrm{d}V_t^0 &= \kappa(\bar{v} - V_t^0)\,\mathrm{d}t + \varepsilon\sqrt{V_t^0}\,\mathrm{d}W_t^{V^0}, \end{aligned}$$

with $\mathrm{d}W^X\,\mathrm{d}W^{V^0} = \rho\,\mathrm{d}t$ and initial condition $(X_0^0, V_0^0) = (X_0, V_0)$. Similarly, $\mathcal{L}_{X_T^J}(u)$ is the Laplace transform of X_T^J in the SVJJ model

$$\begin{aligned} \mathrm{d}X_t^J &= -\frac{1}{2}V_t^J\,\mathrm{d}t + \sqrt{V_t^J}\,\mathrm{d}W_t^J + \mathrm{d}Z_t^X, \\ \mathrm{d}V_t^J &= -\kappa V_t^J\,\mathrm{d}t + \varepsilon\sqrt{V_t^J}\,\mathrm{d}W_t^{V^J} + \mathrm{d}Z_t^V, \end{aligned}$$

with $\mathrm{d}W^J\,\mathrm{d}W^{V^J} = \rho\,\mathrm{d}t$ and initial condition $(X_0^J, V_0^J) = (0,0)$. Therefore, the law of the SVJJ log-price X_T is the convolution of the laws of X_T^0 and X_T^J. del Baño Rollin *et al.* (2010) show that for the Heston log-price X_T^0, it holds that

$$\int_{-\mathrm{i}\infty}^{+\mathrm{i}\infty} |u|^k |\mathcal{L}_{X_T^0}(u)|\,\mathrm{d}u < \infty, \quad \forall\, k \in \mathbb{N},$$

implying that X_T^0 has density function $f_{X_T^0}$ of class $\mathcal{C}^\infty$. In virtue of the convolution representation (46), it also holds that

$$\int_{-\mathrm{i}\infty}^{+\mathrm{i}\infty} |u|^k |\mathcal{L}_{X_T}(u)|\,\mathrm{d}u \le \int_{-\mathrm{i}\infty}^{+\mathrm{i}\infty} |u|^k |\mathcal{L}_{X_T^0}(u)|\,\mathrm{d}u,$$

and we may conclude that the SVJJ log-price X_T has density function f_{X_T} of class $\mathcal{C}^\infty$. ■

Having established the existence of the target density f_{X_T}, the projection coefficients c_n, $n = 1, \ldots, N$ given in (27) require the moments of f_{X_T} up to the approximation order N. The computation of moments and cross-moments of (X_T, V_T) is particularly efficient under SVJJ dynamics, as the process pair $(X_t, V_t)_{t\ge 0}$ belongs to the class of polynomial models introduced in Cuchiero *et al.* (2012). In a nutshell, polynomial processes are Markov processes with infinitesimal generator $\mathcal{A}$ mapping polynomials of degree N into the space of polynomials of degree N or lower. For the SVJJ dynamics (2), the generator $\mathcal{A}$ is given by

$$\begin{aligned} \mathcal{A}f(x,v) = {} & (\kappa\bar{v} - \kappa v)\frac{\partial f}{\partial v} - \left(\bar{\mu} + \frac{1}{2}v\right)\frac{\partial f}{\partial x} \\ & + \frac{v}{2}\left(\frac{\partial^2 f}{\partial x^2} + \varepsilon^2\frac{\partial^2 f}{\partial v^2}\right) + \rho\varepsilon v\frac{\partial^2 f}{\partial v \partial x} \\ & + \lambda\int_{\mathbb{R}\times\mathbb{R}_+} [f(x+\xi_1, v+\xi_2) - f(x,v)] \\ & F_J(\mathrm{d}\xi_1, \mathrm{d}\xi_2), \end{aligned}$$

where F_J is the joint distribution function of the jump sizes (J^X, J^V). Fix now a basis for the space of bivariate polynomials of degree at most N, e.g. the reverse lexicographically ordered bivariate monomials

$$\{b_1, \ldots, b_D\} = \{1, x, v, x^2, xv, v^2, \ldots, xv^{N-1}, v^N\},$$

$$D = \binom{N+2}{2},$$

and compute the $D \times D$ matrix A such that

$$\mathcal{A}b_j = \sum_{i=1}^{D} A_{j,i} b_i, \quad \forall\, j = 1, \ldots, D. \tag{47}$$

For example, the matrix A in the basis $\{1, x, v, x^2, xv, v^2\}$ for polynomials of degree up to $N = 2$, reads as follows

$$A = \begin{pmatrix} 0 & 0 & & & \\ \lambda M(1,0) - \bar{\mu} & 0 & & & \\ \lambda M(0,1) + \kappa\bar{v} & -\kappa & & & \\ \lambda M(2,0) & 2\lambda M(1,0) - 2\bar{\mu} & & & \\ \lambda M(1,1) & \kappa\bar{v} + \lambda M(1,0) & & & \\ \lambda M(0,2) & 0 & & & \end{pmatrix}$$
$$\begin{pmatrix} 0 & 0 & 0 & 0 \\ -\frac{1}{2} & 0 & 0 & 0 \\ 0 & 0 & 0 & 0 \\ 1 & 0 & -1 & 0 \\ \rho\varepsilon - \bar{\mu} + \lambda M(1,0) & 0 & -\kappa & -\frac{1}{2} \\ 2\kappa\bar{v} + \varepsilon^2 + 2\lambda M(0,1) & 0 & 0 & -2\kappa \end{pmatrix},$$

where $M(i,j) = \mathbb{E}[(J^X)^i (J^V)^j]$ denotes the moments and cross-moments of the jump-sizes (J^X, J^V).

The tractability of the polynomial machinery now arises from the fact that all moments and cross-moments $\mathbb{E}[X_T^n V_T^m]$ with order $m + n \le N$ may be computed in a single swipe as follows

$$\begin{aligned} & \mathbb{E}\left[\left(1, X_T, \ldots, X_T^n V_T^m, \ldots, V_T^N\right)^\top\right] \\ & = e^{TA}\left(1, X_0, \ldots, X_0^n V_0^m, \ldots, V_0^N\right)^\top, \end{aligned} \tag{48}$$

where A is the matrix defined in (47) and X_0, V_0 are the initial values of the log-price and variance processes. As such, moment computations in polynomial models merely boils down to computing the matrix exponential of A, which is generally simple and efficient to implement. For more details on polynomial processes and their moment computations, we refer to Cuchiero *et al.* (2012) and Filipović and Larsson (2020).

We now focus on the SVJJ-G model and we turn to the issue of selecting an appropriate reference measure ν for the target log-price f_{X_T}. Rather than searching for a flexible distribution with explicit density, we exploit the structural similarities between the SVJJ-G and the SVJJ-E models, which differ uniquely in the specification of the distribution of the variance jump J^V. As illustrated in Section 2.3, the SVJJ-E model does not perform as well as the SVJJ-G model when calibrated to data. However, the SVJJ-E log-price, here denoted by $\widetilde{X}_T$, resembles the target SVJJ-G log-price X_T closely enough to serve as reference distribution ν for the orthogonal polynomial expansions. Proposition 4.1 ensures the existence of the reference density $f_{\widetilde{X}_T}$, and the moments of $\widetilde{X}_T$ may be computed similarly to the moments of X_T, via the polynomial processes methodology illustrated above. Most importantly, the reference SVJJ-E log-price $\widetilde{X}_T$ has Laplace transform

$\mathcal{L}_{\widetilde{X}_T}$ which only contains elementary functions, hereby allowing for the efficient computation of the pseudo-SPX prices according to Lemma 2.1, as explained in Section 3.2.

In contrast to the example provided in Section 4.1, we do not specify the parameters of the reference $\widetilde{X}_T$ according to the principle of matching moments between the reference and the target distributions. Instead, we simply match one-to-one the parameters common to the two models. Concretely, for a given SVJJ-G parameter set $\Theta = \{\kappa, \bar{v}, \varepsilon, \lambda, \theta, \eta, \mu_x, \sigma_x, \rho_J, \rho\}$, we choose ν to be the log-price $\widetilde{X}_T$ in the SVJJ-E model with transferred parameters $\widetilde{\Theta} = \{\kappa, \bar{v}, \varepsilon, \lambda, \eta, \mu_x, \sigma_x, \rho_J, \rho\}$. A strong advantage of the parameter transfer as opposed to moment matching, is that no additional computations and—possibly time consuming—numerical procedures are required to choose the reference parameter set $\widetilde{\Theta}$. Furthermore, the parameter-transfer ensures that the target and the reference densities share the same tail behavior, a feature suggesting the convergence of the SVJJ-E weighted polynomials to the exact SVJJ-G density. As discussed in Remark 2, Section 3.1, under sufficient regularity conditions, the tail behavior of a density on the real line can be inferred from its critical exponential moments. In Appendix 2, we provide a brief account on critical moments under general SVJJ dynamics. In particular, from Proposition A.1 we see that the exponential critical moments $u^{+/-}_{X_T}$ of the target density f_{X_T} as well as the exponential critical moments $u^{+/-}_{\widetilde{X}_T}$ of the reference density $f_{\widetilde{X}_T}$ are finite for all $T > 0$. Furthermore, under the parameter-transfer described above, it holds that $u^{+}_{X_T} = u^{+}_{\widetilde{X}_T} > 1$ and $u^{-}_{X_T} = u^{-}_{\widetilde{X}_T} < 0$ for all $T > 0$ and therefore the heuristic convergence condition (34) is trivially satisfied.

Naturally, to formalize the reasoning above, one ought to provide a rigorous proof of statement (33). For the Heston model, such a result can be found e.g. in Friz *et al.* (2011), where the tails of the log-price densities are studied in detail. See also Appendix 1 where we utilize such results to show the convergence of gamma-weighted polynomials to the Heston marginal densities.

At the best of our knowledge, a thorough analysis of the tails under general SVJJ dynamics is yet to be carried out and it is out of the scope of the present work. Thus, we conclude the discussion on the convergence of the SVJJ-E weighted polynomials to the exact SVJJ-G density with the heuristic argument provided above.

4.2. Approximating VIX option prices

We now turn the attention to the approximation of VIX call prices under SVJJ-G dynamics. Recall that rather than the VIX itself, the relevant underlying quantity is VIX^2, which, according to (12), is given by an affine transformation of the instantaneous variance V . The properties of the jump-augmented CIR process describing V are studied in detail by Jin *et al.* (2016). Lemmas 3.1 and 3.2 therein, which we summarize in Proposition 4.2 below, provide the results relevant for this work.

PROPOSITION 4.2 *Consider the general SVJJ dynamics (2). Then, at any time $T > 0$ the variance distribution V_T is absolutely continuous with respect to the Lebesgue measure and its density function f_{V_T} can be represented as the Lebesgue-Stieltjes convolution*

$$f_{V_T}(x) = \int_0^x f_{V_T^0}(x - y)\, \mathrm{d}F_{V_T^J}(y), \tag{49}$$

where

- *$f_{V_T^0}$ is the T-time marginal density of the CIR process*

$$\mathrm{d}V_t^0 = \kappa(\bar{v} - V_t^0)\,\mathrm{d}t + \varepsilon\sqrt{V_t^0}\,\mathrm{d}W_t^{V^0}, \tag{50}$$

  with initial condition $V_0^0 = V_0$.
- *$F_{V_T^J}$ is the T-time marginal distribution of the affine process*

$$\mathrm{d}V_t^J = -\kappa V_t^J\,\mathrm{d}t + \varepsilon\sqrt{V_t^J}\,\mathrm{d}W_t^{V^J} + \mathrm{d}Z_t^V,$$

  with initial condition $V_0^J = 0$. In particular, $F_{V_T^J}$ is distributed according to a compound Poisson law.

From Proposition 4.2, it follows immediately that the target VIX_T^2 distribution has density

$$f_{\text{VIX}_T^2}(x) = \frac{1}{a} f_{V_T}\left(\frac{x - b}{a}\right),$$

where a and b are given in (12). Also, the moments of VIX_T^2 are readily available as

$$\mathbb{E}\left[(\text{VIX}_T^2)^n\right] = \sum_{k=0}^{n} \binom{n}{k} a^k b^{n-k} \mathbb{E}\left[V_T^k\right],$$

where the variance moments $\mathbb{E}[V_T^k]$ have already been computed according to (48) to approximate the log-price density X_T.

It only remains to choose the reference measure ν. We could proceed similarly to the log-price case and consider the distribution of the squared VIX arising from the SVJJ-E model. However, the distinction between the exponential and gamma jumps has a much bigger impact on VIX options and futures rather than on SPX options. In our experience, the accuracy of the approximations improves if we select an alternative reference measure which involves gamma distributed jumps. Specifically, we draw inspiration from the convolution representation (49) of the exact variance distribution V_T and consider the following variance density

$$f_{\widetilde{V}_T}(x) = \int_0^x f_{V_T^0}(x - y)\, \mathrm{d}F_{Z_T^V}(y),$$

where $f_{V_T^0}$ is the T-time marginal of the CIR process given in (50) while $F_{Z_T^V}$ is the T-time marginal distribution of the compound Poisson process Z^V. In other words, we introduce a reference variance process $\widetilde{V}$

$$\widetilde{V}_t = V_t^0 + Z_t^V, \tag{51}$$

which can be represented as a sum of a CIR process V^0 and an independent compound Poisson process Z^V with gamma

jump-size. Similarly to the log-price case, all the parameters of V^0 and Z^V are simply transferred from the true variance process V . Finally, we set the reference measure ν as the distribution of the corresponding squared VIX, i.e.

$$\nu \sim \widetilde{\mathrm{VIX}}_T^2 = a\widetilde{V}_T + b,$$

where also the parameters a and b are transferred from the target $\mathrm{VIX}_T^2 = aV_t + b$. The reference density $f_{\widetilde{\mathrm{VIX}}_T^2}$ is the given by

$$f_{\widetilde{\mathrm{VIX}}_T^2}(x) = \frac{1}{a} f_{\widetilde{V}_T}\left(\frac{x-b}{a}\right),$$

while the corresponding Laplace transform $\mathcal{L}_{\widetilde{\mathrm{VIX}}_T^2}$ reads as follows

$$\mathcal{L}_{\widetilde{\mathrm{VIX}}_T^2}(u) = e^{bu}\mathcal{L}_{\widetilde{V}_T}(au) = e^{A_V(T,au)+B_V(T,au)V_0} e^{\lambda T\left(\mathcal{L}_{J^V}(au)-1\right)},$$

where A_V and B_V are specified as in (13) and $\mathcal{L}_{J^V}(u) = (\frac{\eta}{\eta-u})^\theta$ is the Laplace transform of the gamma distributed jump-size.

To compute the reference moments, we notice that both V^0 and Z^V are univariate polynomial processes with generators

$$\mathcal{A}_{V^0} f(v) = (\kappa\bar{v} - \kappa v)\frac{\mathrm{d}f}{\mathrm{d}v} + \frac{v\varepsilon^2}{2}\frac{\mathrm{d}f}{\mathrm{d}v^2},$$
$$\mathcal{A}_{Z^V} f(v) = \lambda \int_0^\infty [f(v+\xi) - f(v)] f_{J^V}(\xi)\,\mathrm{d}\xi,$$

where $f_{J^V}(\xi) = \frac{\eta^\theta}{\Gamma(\theta)}\xi^{\theta-1}e^{-\eta\xi}$ is the density of the gamma jump-size. Hence, we may apply the technique illustrated in Section 4.1 above and compute the moments of V_T^0 and Z_T^V as follows

$$\mathbb{E}\left[\left(1, V_T^0, (V_T^0)^2, \ldots, (V_T^0)^N\right)^\top\right]$$
$$= e^{TA_{V^0}}\left(1, V_0^0, (V_0^0)^2, \ldots, (V_0^0)^N\right)^\top,$$
$$\mathbb{E}\left[\left(1, Z_T^V, (Z_T^V)^2, \ldots, (Z_T^V)^N\right)^\top\right]$$
$$= e^{TA_{Z^V}}\left(1, Z_0^V, (Z_0^V)^2, \ldots, (Z_0^V)^N\right)^\top,$$

where the matrices A_{V^0} and A_{Z^V} are computed according to (47) using the respective generators $\mathcal{A}_{V^0}$ and $\mathcal{A}_{Z^V}$. In virtue of the independence between V^0 and Z^V, the moments of the reference density are then given as follows

$$\mathbb{E}\left[(\widetilde{\mathrm{VIX}}_T^2)^n\right]$$
$$= \sum_{k=0}^n \binom{n}{k} a^k b^{n-k}\mathbb{E}\left[\widetilde{V}_T^k\right]$$
$$= \sum_{k=0}^n \binom{n}{k} a^k b^{n-k}\sum_{\ell=0}^k \binom{k}{\ell}\mathbb{E}\left[\left(V_T^0\right)^\ell\right]\mathbb{E}\left[\left(Z_T^V\right)^{k-\ell}\right].$$

Finally, we conclude with a discussion on the convergence of the proposed approximation to the exact VIX_T^2 density. Clearly, the convergence is guaranteed if condition (26) is satisfied by the target variance density $f_{V_T}(x)$ and the reference variance density $f_{\widetilde{V}_T}(x)$. Once again, we rely on the heuristic arguments provided in Remark 2, Section 3.1. In this case, the convergence condition (37) involves the critical upper exponential moments and the critical negative moments of the target and the reference. From expressions (A2) and (A3) in Appendix 2 we obtain that for the target variance density f_{V_T}, the critical upper exponential moment is given by

$$u_{V_T}^+ = \min\left\{\eta, \frac{2\kappa\eta}{(1-e^{-\kappa T})\varepsilon^2\eta + 2\kappa e^{-\kappa T}}\right\},$$

while for the reference variance density $f_{\widetilde{V}_T}(x)$

$$u_{\widetilde{V}_T}^+ = \min\left\{\eta, u_{V_T^0}^+\right\} = \min\left\{\eta, \frac{2\kappa}{(1-e^{-\kappa T})\varepsilon^2}\right\}.$$

We see that, in whole generality, $u_{\widetilde{V}_T}^+ \geq u_{V_T}^+$ for all $T > 0$. However, for common parameter values—and in particular in all the calibrations we carry out—it holds that $u_{V_T}^+ = u_{\widetilde{V}_T}^+ = \eta$, implying that the right tail of f_{V_T} and $f_{\widetilde{V}_T}$ decay at the same exponential rate. Furthermore, Proposition A.2 entails that

$$q_{V_T}^- = q_{\widetilde{V}_T}^- = -\frac{2\kappa\bar{v}}{\varepsilon^2}.$$

We may therefore conclude that $f_{V_T}(x)$ and $f_{\widetilde{V}_T}(x)$ typically fulfill the heuristic convergence condition (37).

4.3. *Numerical tests*

We now proceed to test the robustness and the accuracy of the approximations proposed in Sections 4.1 and 4.2. We start by analysing the convergence of the approximate SPX and VIX implied volatilities to the exact SVJJ-G curves at a fixed maturity. We consider two different sets of parameters resulting from the SVJJ-G calibrations performed in Section 2.3 on the dates 21/03/2018 and 22/05/2020. The concrete parameters may be found in table 2. Similarly to the experiment illustrated in figure 3, the two sets discriminate between a low volatility scenario (2018) and more distressed market conditions (2020). We fix the maturity at $T = 3$ months and a SPX log-moneyness $\log(K/S_0)$ interval ranging from -0.8 up to 0.5. For VIX options, we consider a strike interval $K \in [20, 40]$ around the exact futures price of $F = 22.13$ for the 21/03/2018, and $K \in [25, 45]$ for the 22/05/2020 where the exact futures price is $F = 31.70$. We implement price approximations for orders $N \in \{0, 3, 5, 10\}$ and we plot the corresponding implied volatilities against the exact curves in figure 4.

We note that for SPX implied volatilities, the order $N = 0$—corresponding to the plain SVJJ-E model—yields already a decent approximation under both parameter specifications. That is clearly not the case for VIX implied volatilities. This is due to the fact that the approximate VIX implied volatilities are obtained by inverting the Black formula (20) at the corresponding approximate VIX futures prices. In other words, both the N-order errors of VIX option prices as well as the N-order errors of VIX futures prices affect the N-order implied volatility computations. At $N = 0$ the approximations are simply to rough to yield sensible results. However, it is apparent

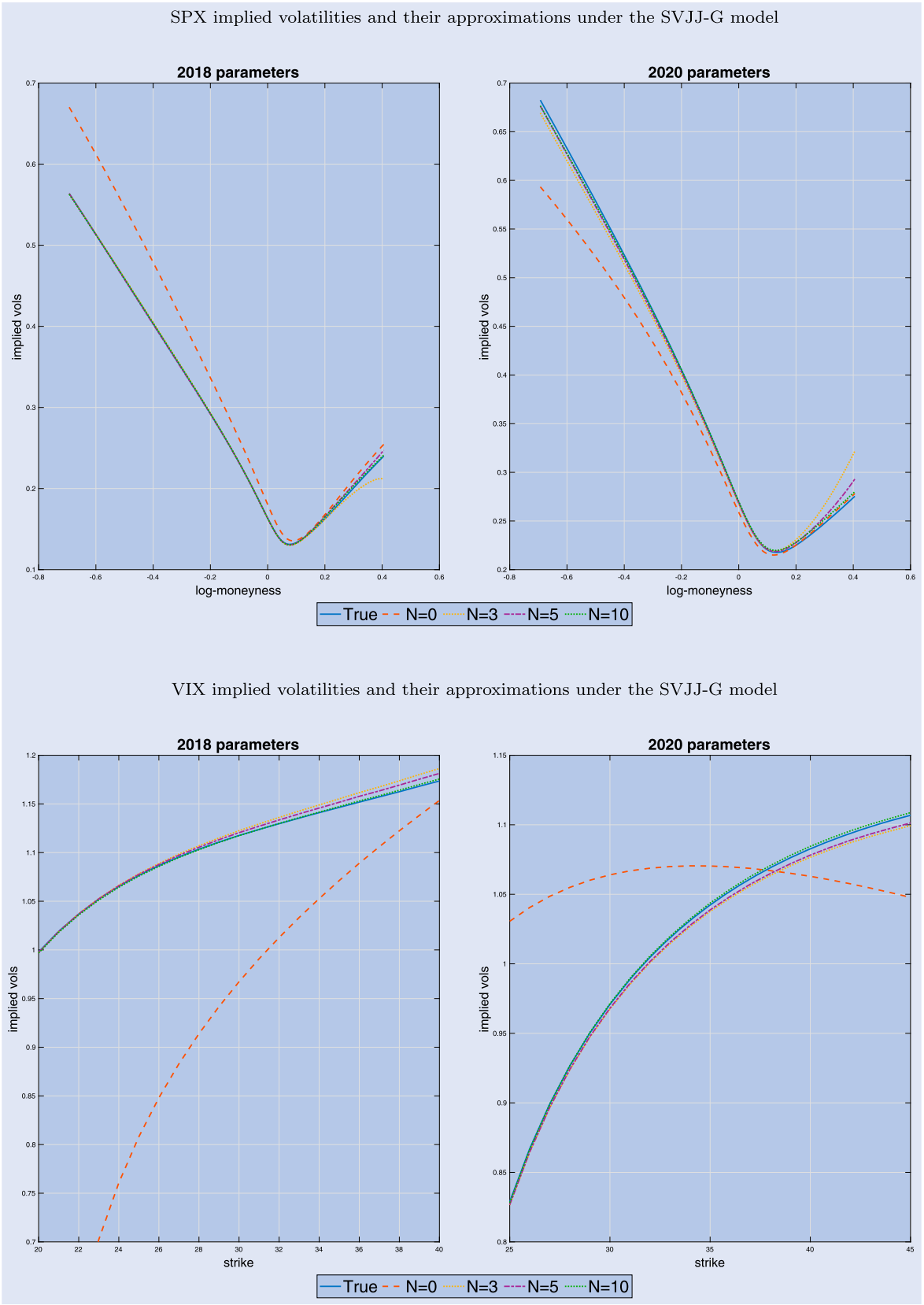

Figure 4. SPX (top panel) and VIX (bottom panel) implied volatilities in the SVJJ-G model for parameter sets corresponding to the 2018 calibration (left panel) and the 2020 calibration (right panel). The curves correspond to price approximations of order $N = 0,3,5,10$ benchmarked against the exact SVJJ-G implied volatilities. The VIX futures prices are $F = 22.13$ and $F = 31.70$ in 2018 and 2020, respectively.

that bothe for SPX and VIX options the approximate implied volatilities are very accurate already at order $N=5$, under both parameter scenarios. The higher order $N=10$ only provides slight improvements. The experiment indicates not only that the heuristic convergence arguments discussed in Sections 4.1 and 4.2 above are likely to hold, but also that the convergence is attained already at low orders.

Next, we test the accuracy of the approximation not only for fixed maturity curves but throughout the entire volatility surfaces. Specifically, we conduct a calibration experiment within a controlled environment: We generate SPX and VIX surfaces of exact SVJJ-G option prices and then we calibrate the approximations to these surfaces using the objective function (19). It is well-known that calibration using a numerical optimization procedure is a delicate task as such problems are highly non-linear and susceptible to many local minima. To facilitate such difficulties, we carry out the following two-step procedure.

(i) Perform the calibration starting at a low approximation order $N=3$.
(ii) Re-do the calibration starting from the solution obtained in the first step, but at a higher approximation order. Here we set $N=5$ so to achieve a reasonable tradeoff between accuracy and efficiency we set $N=5$.

The first step is to zone in on a good local minimum, while the second step increases the accuracy to obtain the best possible optimum. It is our experience that this procedure is better than simply starting the full calibration at the higher order. Once again we consider two different volatility scenario, but

Table 6. Calibration results from the controlled environment experiment corresponding to low volatility (top panel) and high volatility (bottom panel).

	κ	$\bar{v}$	ε	λ	θ	η	μ_x	σ_x	ρ	ρ_J
True	2	0.05	0.4	0.1	1.2	2	−0.05	0.1	−0.7	−0.2
Calibrated	2.04	0.0499	0.40	0.103	1.20	2.03	−0.021	0.078	−0.68	−0.26
True	5	0.15	1.4	0.1	0.75	1.2	−0.05	0.1	−0.9	−0.2
Calibrated	5.07	0.150	1.39	0.103	0.79	1.2	−0.017	0.094	−0.91	−0.23

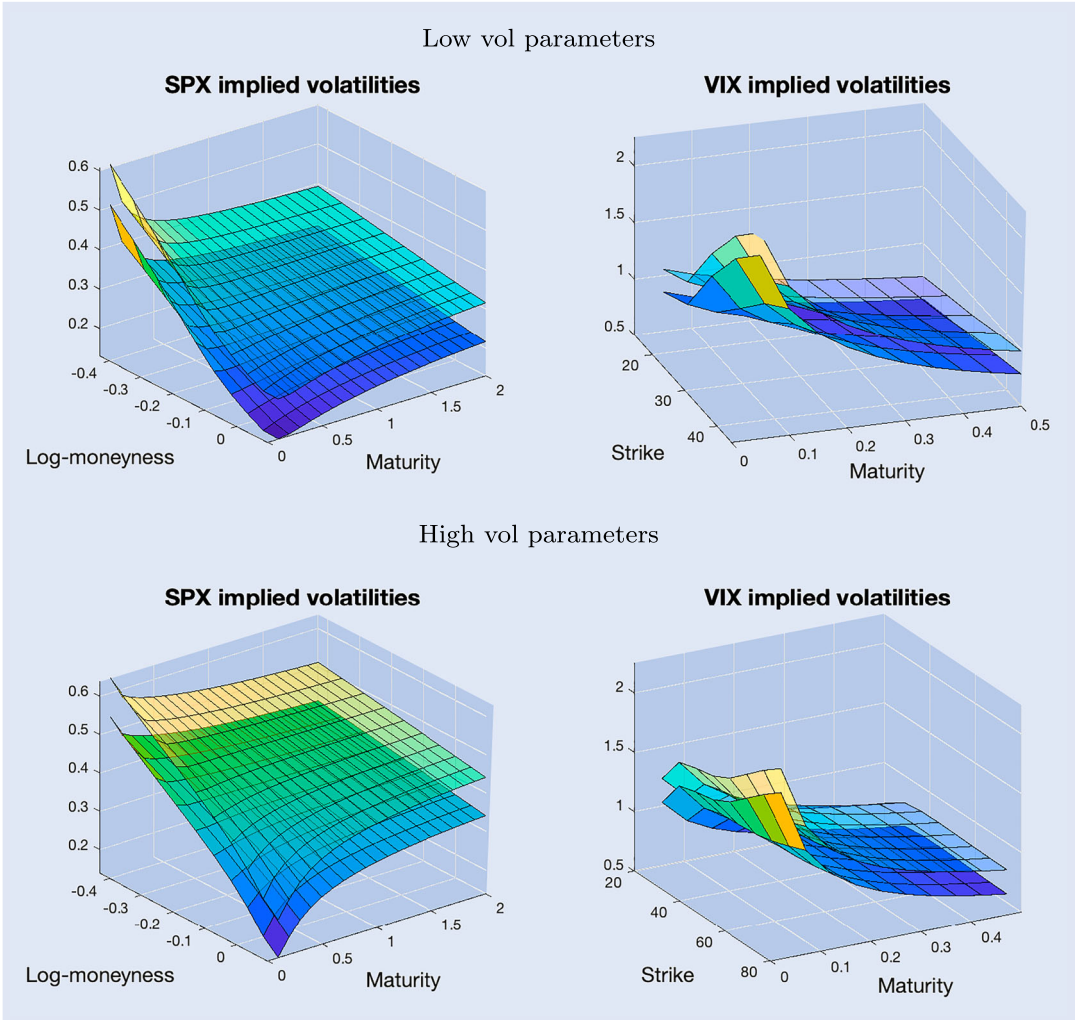

Figure 5. Implied volatility surfaces from the controlled environment experiment for the different parameter sets. The true surfaces are non-transparent and the calibrated surfaces are transparent. SPX and VIX surfaces are shifted by 0.1 and 0.2 respectively. SPX implied volatilities are plotted against log-moneyness $\log(K/S_0)$.

Table 7. Calibrated parameters in the SVJJ-G model using the exact versus the approximation method.

	κ	$\bar{v}$	ε	λ	θ	η	μ_X	σ_X	ρ	ρ_J
2018										
Exact	4.99	0.020	0.80	0.106	1.80	1.31	0.01	0.12	− 0.64	− 0.28
Approx.	4.89	0.020	0.82	0.104	1.73	1.32	0.00	0.14	− 0.69	− 0.27
2019										
Exact	5.27	0.033	0.72	0.047	0.34	0.45	− 0.04	0.16	− 0.68	− 0.28
Approx.	5.37	0.033	0.67	0.047	0.36	0.44	− 0.05	0.16	− 0.64	− 0.30
2020										
Exact	4.50	0.084	1.58	0.119	1.64	1.24	0.09	0.13	− 0.78	− 0.22
Approx	4.48	0.084	1.55	0.122	1.58	1.27	0.08	0.13	− 0.80	− 0.20

Note: The ARPE's are computed by plugging the parameters into the exact pricing formula.

Table 8. Data calibration times in seconds.

Exp. exact	Gamma exact	Gamma approx.
205	1541	263

to differentiate from the previous experiment, we consider two new parameter sets. The true and the calibrated parameters are displayed in table 6 while figure 5 shows the corresponding implied volatility surfaces. We see that the true parameters are generally closely matched, except perhaps for the jump parameter μ_x. However, as seen on figure 5, the resulting implied volatility surfaces are virtually indistinguishable.

4.4. Calibration to data

As the final test, we see how well the proposed approximations fare when taken to data. Specifically, we perform the exact same calibrations as in Section 2.3 on the dates 21/03/2018, 07/01/2019 and 22/05/2020, but using the approximating pricing methodology instead of the exact. Ideally, we wish to obtain the same optimum in both calibrations. In table 7 we provide the parameter estimates obtained via the two calibrations. The corresponding implied volatilities are shown in figures A3, A4 and A5 in Appendix 3.

We see that the approximation-based calibration is able to retrieve parameters quite close to the ones found in the exact calibration, albeit with some slight deviation, particularly in the jump parameters. This leads to slightly higher pricing errors, particularly for the VIX implied volatilities. Given that the approximations are by definition not exact, there might be points that yield a lower value for the objective function than at the optimum found by the exact formula, i.e. the calibrated optimum will always be an approximate optimum as well. Overall we conclude that the obtained optimum is very close to the desired point and we find that the approximations are able to provide close calibration results as compared to a calibration using exact transform inversion methods. The computational burden, however, in significantly lower. The computational time of the calibrations based on the approximations compared to the calibrations in Section 2.3 is shown in table 8. It follows that the approximations allow for calibrating the SVJJ-G model accurately to data with a computational time comparable to that of the SVJJ-E model.

5. Summary and conclusions

We have investigated the impact of the jump distribution on the joint calibration to SPX and VIX option prices for a selection of models from the SVJJ framework. We run an empirical horse race between the original suggestion of Duffie *et al.* (2000), i.e. the SVJJ-E model with exponential jumps in variance and the SVJJ-G and SVJJ-IG models where variance jumps are distributed as a gamma and an inverse gaussian law respectively. We find that in some days of our sample all three specifications produce rather high calibration errors indicating that the underlying SVJJ dynamics are too simple to consistently provide satisfactory fits. However, we also find that the SVJJ-G model outperforms the SVJJ-E and SVJJ-IG counterparts in each of the calibrations we conduct. Notably, the fit of the SVJJ-G model to VIX implied volatilities yields errors which on average are 20% lower than in the standard SVJJ-E model and 40% lower than in the SVJJ-IG model. Similar results are attained for VIX futures prices. All in all, our results show that in models with affine variance dynamics the choice of the jump distribution can significantly impact the joint calibration performance. The downside of this added flexibility, however, is a severe increase in computational time. To amend for this loss of tractability, we expand on the well-established literature of density approximations and propose a novel combination of Fourier methods and orthogonal polynomial expansions to efficiently and accurately price SPX and VIX options. In particular, we find that we may exploit the tractability of the SVJJ-E model to construct very accurate, robust and fast approximations to option prices within the SVJJ-G model. We test the feasibility of the methodology through a series of numerical experiments and we find that the approximations yield essentially the same results as the exact transform method, but require only a small fraction of the computational time.

Acknowledgments

The authors would like to thank Bent Jesper Christensen, Julien Guyon, Thomas Kokholm, the participants at the XXIV Workshop on Quantitative Finance, and two anonymous referees for useful comments and suggestions.

Disclosure statement

No potential conflict of interest was reported by the author(s).

Funding

This work was supported by the Danish Council for Independent Research under Grant DFF 0133-00151B.

References

Abi Jaber, E. and Li, S., Volatility models in practice: Rough, Path-dependent or Markovian? Preprint, 2024.
Ackerer, D. and Filipović, D., Option pricing with orthogonal polynomial expansions. *Math. Finance*, 2020, **30**, 47–84.
Andersen, L.B.G. and Piterbarg, V.V., Moment explosions in stochastic volatility models. *Finance Stoch.*, 2007, **11**, 29–50.
Asmussen, S. and Bladt, M., Gram-Charlier methods, regime-switching and stochastic volatility in exponential Lévy models. *Quant. Finance*, 2022, **22**, 675–689.
Bardgett, C., Gourier, E. and Leippold, M., Inferring volatility dynamics and risk premia from the S&P 500 and VIX markets. *J. Financ. Econ.*, 2019, **131**, 593–618.
Barletta, A. and Nicolato, E., Orthogonal expansions for VIX options under affine jump diffusions. *Quant. Finance*, 2018, **18**, 951–967.
Bayer, C., Friz, P. and Gatheral, J., Pricing under rough volatility. *Quant. Finance*, 2016, **16**, 887–904.
Bingham, N.H., Goldie, C.M. and Teugels, J.L., *Regular Variation*, Encyclopedia of mathematics and its applications, 1987 (Cambridge University Press: Cambridge).
Bondi, A., Livieri, G. and Pulido, S., Affine Volterra processes with jumps. *Stoch. Process. Appl.*, 2024a, **168**, 104264.
Bondi, A., Pulido, S. and Scotti, S., The rough Hawkes Heston stochastic volatility model. *Math. Finance*, 2024b, **34**, 1197–1241.
Broadie, M. and Jain, A., The effect of jumps and discrete sampling on volatility and variance swaps. *Int. J. Theor. Appl. Finance*, 2008, **11**, 761–797.
Carr, P. and Madan, D.B., A note on sufficient conditions for no arbitrage. *Finance Res. Lett.*, 2005, **2**, 125–130.
CBOE, The CBOE volatility index – VIX. *White Paper*, 2023.
Cont, R. and Kokholm, T., A consistent pricing model for index options and volatility derivatives. *Math. Finance*, 2013, **23**, 248–274.
Cuchiero, C., Keller-Ressel, M. and Teichmann, J., Polynomial processes and their applications to mathematical finance. *Finance Stoch.*, 2012, **16**, 711–740.
Cuchiero, C., Gazzani, G., Möller, J. and Svaluto-Ferro, S., Joint calibration to SPX and VIX options with signature-based models. Preprint, 2023. arXiv:2301.13235.
del Baño Rollin, S., Ferreiro-Castilla, A. and Utzet, F., On the density of log-spot in the Heston volatility model. *Stoch. Process. Appl.*, 2010, **120**, 2037–2063.
Duffie, D., Pan, J. and Singleton, K., Transform analysis and asset pricing for affine jump-diffusions. *Econometrica*, 2000, **68**, 1343–1376.
Filipović, D. and Larsson, M., Polynomial jump-diffusion models. *Stoch. Syst.*, 2020, **10**, 71–97.
Filipović, D., Mayerhofer, E. and Schneider, P., Density approximations for multivariate affine jump-diffusion processes. *J. Econom.*, 2013, **176**, 93–111.
Friz, P., Gerhold, S., Gulisashvili, A. and Sturm, S., On refined volatility smile expansion in the Heston model. *Quant. Finance*, 2011, **11**, 1151–1164.
Guyon, J. and Lekeufack, J., Volatility is (mostly) path-dependent. *Quant. Finance*, 2023, **23**, 1221–1258.
Guyon, J. and Mustapha, S., Neural joint S&P 500/VIX smile calibration. *Risk*, December 2023.
Heston, S.L., A closed form solution for options with stochastic volatility with application to bonds and currency options. *Rev. Financ. Stud.*, 1993, **6**, 327–343.
Jarrow, R. and Rudd, A., Approximate option valuation for arbitrary stochastic processes. *J. Financ. Econ.*, 1982, **10**, 347–369.
Jin, P., Ruediger, B. and Trabelsi, C., Exponential ergodicity of the jump-diffusion CIR process. In *Proceedings of the Stoch. Env. Financ. Econ.*, Vol. 138 of *Springer Proceedings in Mathematics & Statistics*, pp. 285–300, 2016 (Springer Nature: New York).
Keller-Ressel, M., Moment explosions and long-term behavior of affine stochastic volatility models. *Math. Finance*, 2011, **21**, 73–98.
Kokholm, T. and Stisen, M., Joint pricing of VIX and SPX options with stochastic volatility and jump models. *J. Risk Finance*, 2015, **16**, 27–48.
Lian, G.H. and Zhu, S.P., Pricing VIX options with stochastic volatility and random jumps. *Decis. Econ. Finance*, 2013, **36**, 71–88.
Madan, D.B. and Milne, F., Ccontingent claims valued and hedged by pricing and investing in a basis. *Math. Finance*, 1994, **4**, 223–245.
Maneesoonthorn, W., Forbes, C.S. and Martin, G.M., Inference on self-exciting jumps in prices and volatility using high-frequency measures. *J. Appl. Econom.*, 2017, **32**, 504–532.
Neuberger, A., The log contract. *J. Portf. Manag.*, 1994, **20**, 74–80.
Nicolato, E., Pisani, C. and Sloth, D., The impact of jump distributions on the implied volatility of variance. *SIAM J. Financ. Math.*, 2017, **8**, 28–53.
Pacati, C., Pompa, G. and Renó, R., Smiling twice: The Heston + + model. *J. Bank. Finance*, 2018, **96**, 185–206.
Ribeiro, A. and Poulsen, R., Approximation behoves calibration. *Quant. Finance Lett.*, 2013, **1**, 36–40.
Rømer, S.E., Empirical analysis of rough and classical stochastic volatility models to the SPX and VIX markets. *Quant. Finance*, 2022, **22**, 1805–1838.
Schmelzle, M., Option pricing formulae using fourier transform: Theory and application. Preprint, 2010.
Sepp, A., VIX option pricing in a jump-diffusion model. *Risk*, 2008, **21**, 84–89.
Szegö, G., *Orthogonal Polynomials*, Vol. XXIII, 1939 (American Mathematical Society; Colloquium publications: Providence, RI).
Willems, S., Asian option pricing with orthogonal polynomials. *Quant. Finance*, 2019, **19**, 605–618.

Appendices

Appendix 1. Convergence of variance gamma-weighted polynomials to the Heston density

Let X_T^0 denote the log-price at time T under Heston dynamics and let $f_{X_T^0}$ be its density. Friz *et al.* (2011) show that the tails of $f_{X_T^0}$ behave as follows

$$f_{X_T^0}(x) \sim e^{-u_H^+ x} e^{A\sqrt{x}} x^{B-3/4} \left(1 + O(x^{-1/2})\right), \quad x \to +\infty,$$

$$f_{X_T^0}(x) \sim e^{-u_H^- x} e^{A\sqrt{|x|}} |x|^{C-3/4} \left(1 + O(|x|^{-1/2})\right), \quad x \to -\infty,$$

where A, B and C are positive constants while u_H^+ and u_H^- are the critical exponential moments

$$u_H^+ = \sup\left\{u \in \mathbb{R} : \mathbb{E}\left[e^{uX_T^0}\right] < \infty\right\},$$

$$u_H^- = \inf\left\{u \in \mathbb{R} : \mathbb{E}\left[e^{uX_T^0}\right] < \infty\right\}.$$

Following Andersen and Piterbarg (2007) (see also Keller-Ressel 2011), u_H^+ and u_H^- can be numerically computed as the

Table A1. The moment matched *VG* parameters and the critical exponential moments of ϕ_{VG} and $f_{X_T^0}$ in the Heston model with $\varepsilon = 0.22$ (low vol-of-vol) and $\varepsilon = 0.8$ (high vol-of vol).

	μ	α	β	ν	u^+_{VG}	u^-_{VG}	u^+_H	u^-_H
low vol-of-vol	0.23	22.80	− 11.90	0.25	34.70	− 10.89	52.94	− 12.30
high vol-of-vol	0.32	7.12	− 4.65	1.26	11.76	− 2.47	15.76	− 3.15

Note: The common parameters are $\kappa = 1.5$, $\bar{v} = 0.04$, $V_0 = 0.03$, $\rho = -0.75$, while the maturity is $T = 1$.

solutions of

$$T = \frac{2}{\sqrt{-\Delta(u)}} \arctan 2\left(\sqrt{-\Delta(u)}, (\rho\varepsilon u - \kappa)\right),$$

where $\Delta(u) = (\kappa - \rho\varepsilon u)^2 - \varepsilon^2(u^2 - u)$.

Consider now the tails behavior of the reference $V\ G$ density. Applying the limiting form

$$K_\omega(x) \sim \sqrt{\frac{\pi}{2x}} e^{-x}, \quad x \to \infty,$$

to expression (38) we obtain that the tails of $\phi_{VG}(x)$ behave as follows

$$\phi_{VG}(x) \sim x^{\lambda-1} e^{-u^+_{VG}x}, \quad x \to +\infty,$$
$$\phi_{VG}(x) \sim |x|^{\lambda-1} e^{-u^-_{VG}x}, \quad x \to -\infty,$$

where

$$u^+_{VG} = \alpha - \beta \quad u^-_{VG} = -(\alpha + \beta).$$

Clearly, $f_{X_T^0}$ and ϕ_{VG} fulfill the convergence condition (26) whenever

$$u^+_{VG} < 2u^+_H \quad \text{and} \quad u^-_{VG} > 2u^-_H. \tag{A1}$$

In table A1 we report the parameters of the moment-matched reference ϕ_{VG} and the critical exponential moments corresponding to the two Heston parameter-sets under examination. We see that in both the low vol-of-vol and high vol-of-vol scenarios the critical moments fulfill condition (A1), hereby guaranteeing the theoretical convergence of the ϕ_{VG}-weighted polynomials to the target Heston density.

Appendix 2. Critical moments in the SVJJ model

Consider the log-price process X and define the explosion time for the exponential moment of order $u \in \mathbb{R}$ as follows

$$T^*(u) = \sup\left\{t \geq 0 : \mathbb{E}\left[e^{uX_t}\right] < \infty\right\}.$$

The critical exponential moments $u^+_{X_T}$ and $u^-_{X_T}$ defined as in (31) and (32) can be obtained by the generalized inversion of T^*, i.e.

$$u^+_{X_T} = \inf\left\{u > 0 : T^*(u) = T\right\},$$
$$u^-_{X_T} = \sup\left\{u < 0 : T^*(u) = T\right\}.$$

A full description of $T^*(u)$ under general affine stochastic volatility dynamics is provided in Keller-Ressel (2011). Proposition 4.1 therein, tailored to the SVJJ models we consider in this work, reads as follows.

Proposition A.1 *Consider the SVJJ dynamics* (2) *with jump-size distribution specified according to* (17). *Define the functions*

$$\Delta(u) = (\kappa - \rho\varepsilon u)^2 - \varepsilon^2(u^2 - u), \quad w(u) = \frac{(\kappa - \rho\varepsilon u) - \sqrt{\Delta(u)}}{\varepsilon^2},$$

and

$$R(u, w) = \frac{\varepsilon^2}{2} w^2 - (\kappa - \rho\varepsilon u) + \frac{1}{2}(u^2 - u),$$

and let $\mathcal{J}$ *denote the set*

$$\mathcal{J} = \left\{u \in \mathbb{R} : \Delta(u) \geq 0 \text{ and } \mathcal{L}_{J^V}(\rho_J u + w(u)) < \infty\right\}.$$

Assume that $\mathcal{L}_{J^V}(\rho_J u) < \infty$. *Then: If* $u \in \mathcal{J}$ *then*

$$T^*(u) = \infty$$

If $u \notin \mathcal{J}$ *and then*

$$T^*(u) = \int_0^{w^+(u)} \frac{1}{R(u, \eta)}\, \mathrm{d}\eta,$$

where $w^+(u) = \sup\{w \geq 0 : \mathcal{L}_{J^V}(\rho_J u + w) < \infty\}$.

Otherwise, i.e. if $\mathcal{L}_{J^V}(\rho_J u) = \infty$, *then*

$$T^*(u) = 0.$$

Notice that the variance jumps specification J^V affects the explosion times $T^*(u)$ – and therefore the exponential critical moments $u^+_{X_T}$ and $u^-_{X_T}$—only through the domain of existence of $\mathcal{L}_{J^V}$. From (15) and (18), we see that for both the SVJJ-G model and the SVJJ-E model with lifted parameters it holds that $\mathcal{L}_{J^V}(w) < \infty$ for $w < \eta$, and we may conclude that the two models share the same $u^+_{X_T}$ and $u^-_{X_T}$ for any $T \geq 0$.

Consider now the instantaneous variance process V . The positive critical exponential moment

$$u^+_{V_T} = \sup\left\{u \in \mathbb{R} : \mathbb{E}\left[e^{uV_T}\right] < \infty\right\},$$

can be read directly from expressions (13) and it is given by

$$u^+_{V_T} = \min\left\{w^+, \frac{2\kappa w^+}{(1 - e^{-\kappa T})\varepsilon^2 w^+ + 2\kappa e^{-\kappa T}}\right\}, \tag{A2}$$

where $w^+ = \sup\{w \geq 0 : \mathcal{L}_{J^V}(w) < \infty\}$. In particular, letting $w^+ \to \infty$, we obtain for the CIR process V^0, the upper exponential critical moment becomes

$$u^+_{V^0_T} = \frac{2\kappa}{(1 - e^{-\kappa T})\varepsilon^2}. \tag{A3}$$

The behavior of V_T near zero is related the critical negative moment $q^-_{V_T}$ defined in (35), which we proceed to determine in the proposition below.

Proposition A.2 *Consider the variance process V in the general SVJJ dynamics* (2). *Then, for any time* $T > 0$, *and any jump-size* J^V, *the critical negative moment is given by*

$$q^-_{V_T} = -\frac{2\kappa\bar{v}}{\varepsilon^2}.$$

Proof Recall that a positive, measurable function on $\mathbb{R}_+$ is said to be regularly varying at ∞ with index α if the following holds

$$\lim_{x \to +\infty} \frac{f(\xi x)}{f(x)} = \xi^\alpha, \tag{A4}$$

for all $\xi > 0$. In this case we write $f \in \mathcal{R}_\alpha$. Also, recall that for a random variable H on $\mathbb{R}_+$ and $\alpha < 0$, it holds that

$$F_H(1/u) \in \mathcal{R}_\alpha \quad \text{if and only if } \mathcal{L}_H(-u) \in \mathcal{R}_\alpha, \tag{A5}$$

where $F_H(u) = \mathbb{P}(H \leq u)$ denotes the cumulative distribution function of H, while $\mathcal{L}_H(u) = \mathbb{E}[e^{uH}]$ is its Laplace transform. See, e.g. Bingham *et al.* (1987, XIII.5, Theorem 3). In particular, combining (A4) and (A5) with the fact that $\mathbb{E}[H^q]$, with $q < 0$, may be expressed as

$$\mathbb{E}[H^q] = -q \int_0^\infty u^{-q-1} F(1/u)\, \mathrm{d}u,$$

we obtain that if $\mathcal{L}_H(-u) \in \mathcal{R}_\alpha$, the negative critical moment is given by

$$q_H^- = \inf\left\{q \in \mathbb{R} : \mathbb{E}\left[H^q\right] < \infty\right\} = \alpha.$$

Consider the Laplace transform $\mathcal{L}_{V_T^0}$ of the CIR process (50), i.e.

$$\mathcal{L}_{V_T^0}(u) = e^{A_V(T,u) + B_V(T,u)V_0},$$

where the functions A_V, B_V are given in (13). It is immediate to see that $\mathcal{L}_{V_T^0}(-u) \in \mathcal{R}_\alpha$, with $\alpha = -\frac{2\kappa\bar{v}}{\varepsilon^2}$. Consider now the function $\mathcal{L}_{V_T^J}(u) = e^{C_V(T,u)}$, which, according to Proposition 4.2 is the Laplace transform of the compound Poisson distribution $F_{V_T^J}$. Thus, it holds that

$$\lim_{u\to\infty} \mathcal{L}_{V_T^J}(-u) = e^{-\lambda_T^J},$$

where $\lambda_T^J > 0$ is the intensity of $F_{V_T^J}$, implying that

$$\mathcal{L}_{V_T}(-u) = \mathcal{L}_{V_T^0}(-u)\mathcal{L}_{V_T^J}(-u) \in \mathcal{R}_\alpha, \quad \text{with } \alpha = -\frac{2\kappa\bar{v}}{\varepsilon^2},$$

which concludes the proof. ■

Notice that the reasonings above apply to any distribution which can be represented as a convolution of a CIR marginal V_T^0 with a compound Poisson distribution. In particular, we may conclude that also for the reference variance distribution $\widetilde{V}_T$ defined in (51) it holds that $q_{\widetilde{V}_T}^- = -\frac{2\kappa\bar{v}}{\varepsilon^2}$.

Appendix 3. Further calibration results

Here we present the calibration results left out from Sections 2.3 and 4.4. Figures A1 and A2 depict the SPX and VIX implied volatility smiles resulting from the calibrations on the dates 21/03/2018 and 22/05/2020 carried out in Section 2.3. Not all maturities are depicted, but the smiles are representative of the overall picture. Observed implied volatilities are represented by blue circles, while the three different model fits are represented by lines. VIX futures prices are included as vertical lines with colors consistent with the implied volatilities. SPX implied volatilities are plotted against log-moneyness $\log(K/S_0)$.

Figures A3, A4 and A5 depict the volatility surfaces from calibrations based on the approximate pseudo-prices versus those based on exact pricing formulae as described in Section 4.4. Observed implied volatilities are represented by blue circles, while the lines represent the implied volatilities generated by the optima found in the conventional calibration in Section 2.3 versus the approximation based calibration. Both the depicted model surfaces are produced by inverting prices computed via the exact formula.

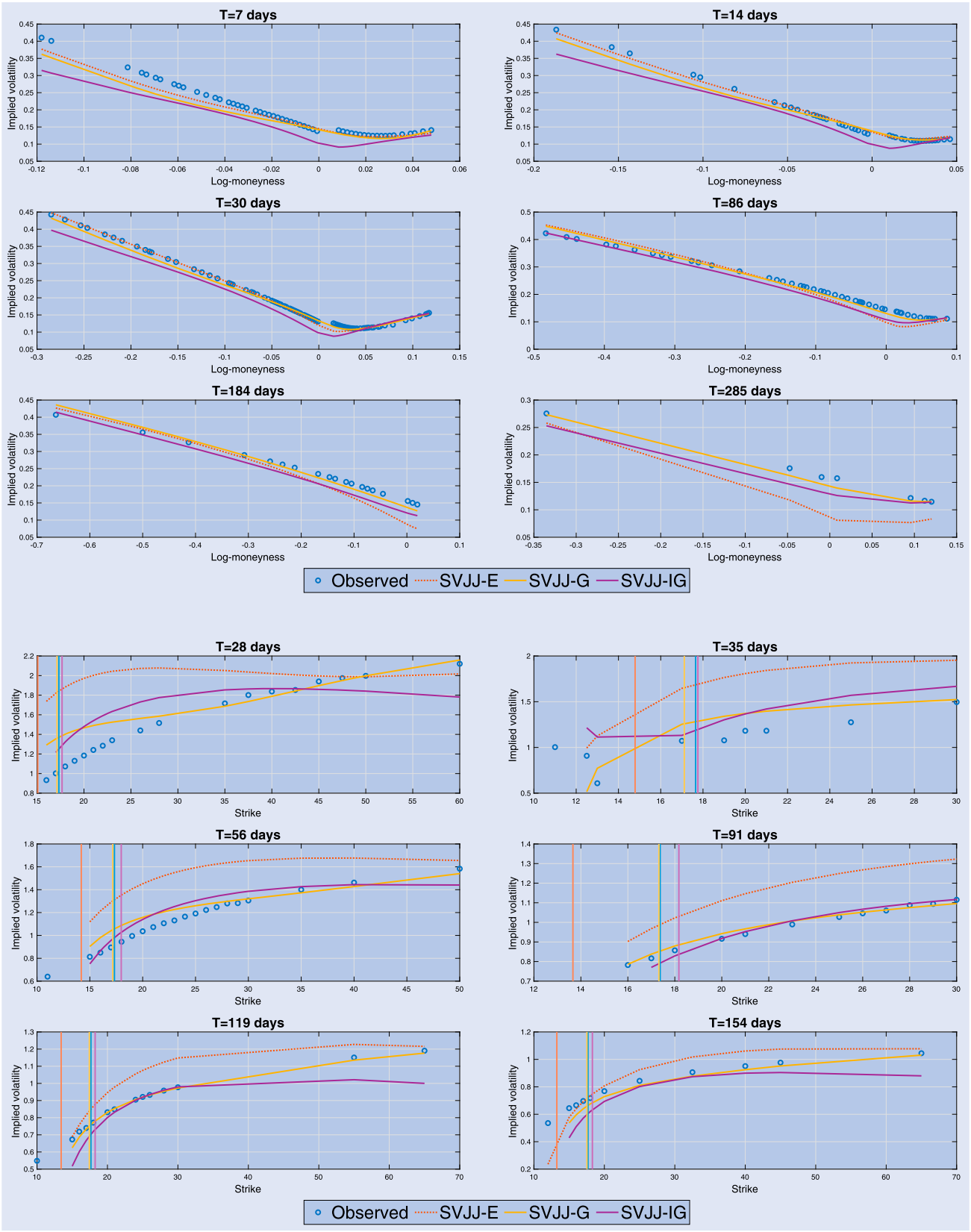

Figure A1. SPX and VIX implied volatility fits on March 21st 2018. VIX futures prices are represented by vertical lines.

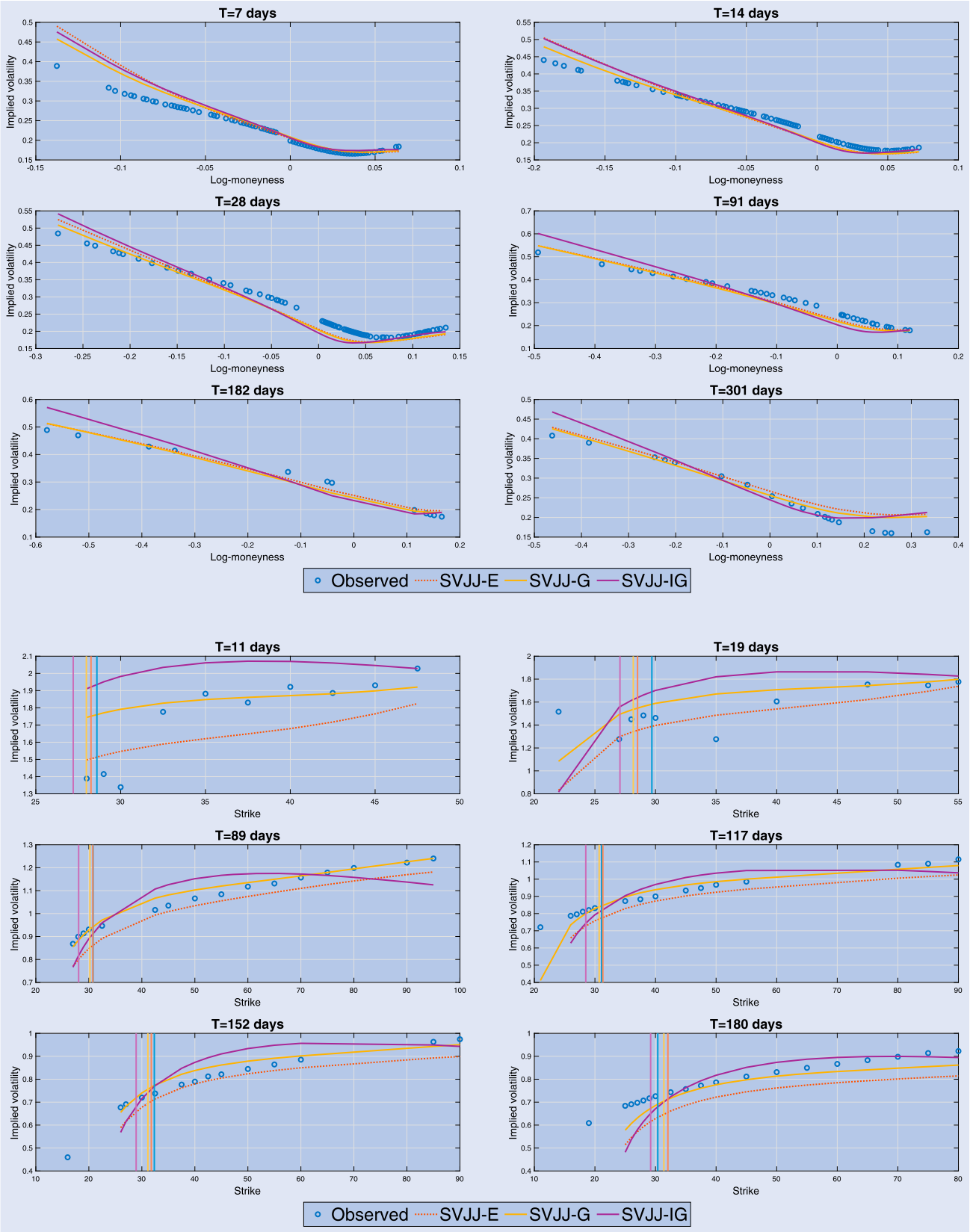

Figure A2. SPX and VIX implied volatility fits on May 22nd 2020. VIX futures prices are represented by vertical lines.

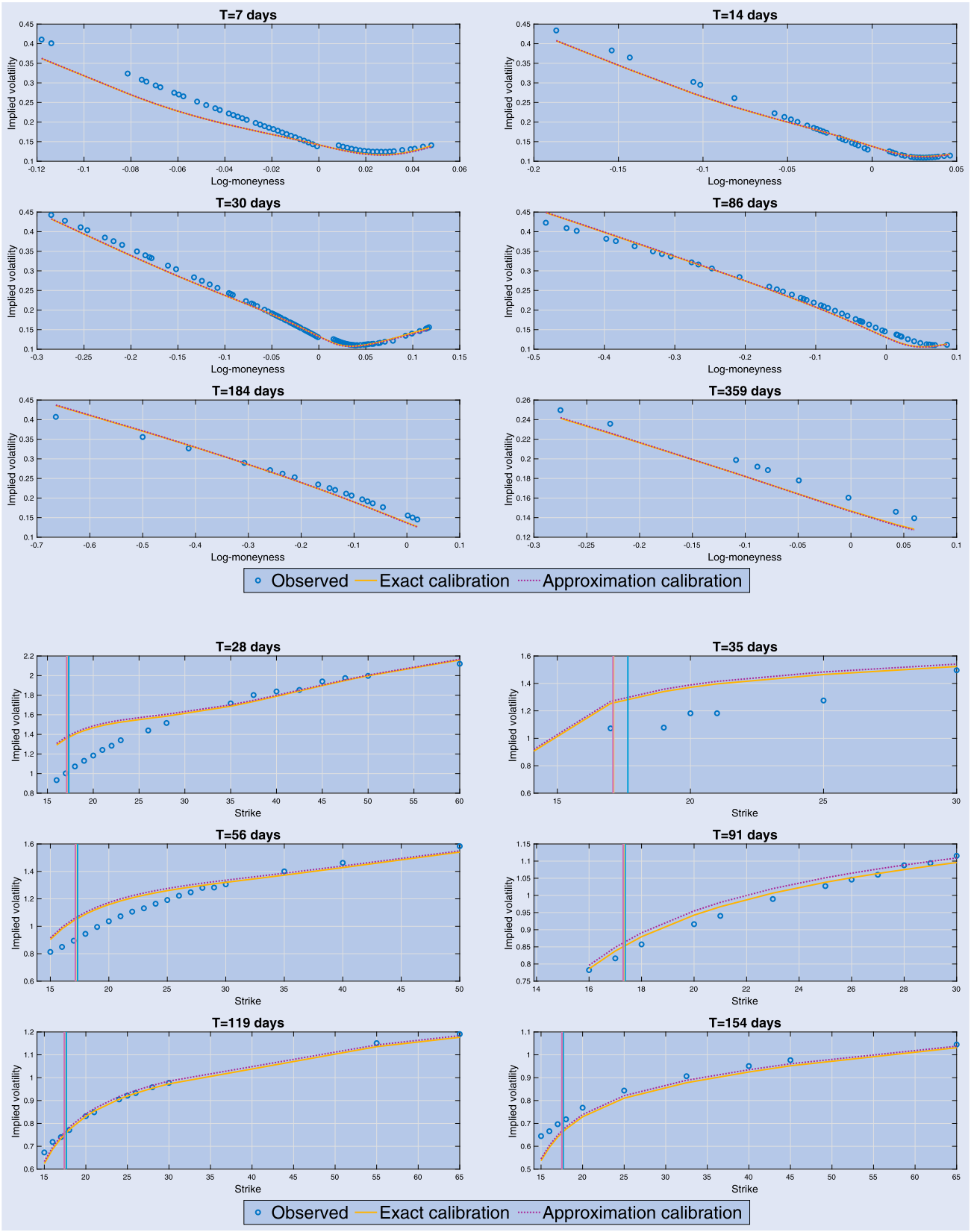

Figure A3. Comparison of SPX implied volatilities on March 21st 2018 between the calibrated approximation and exact pricing formula.

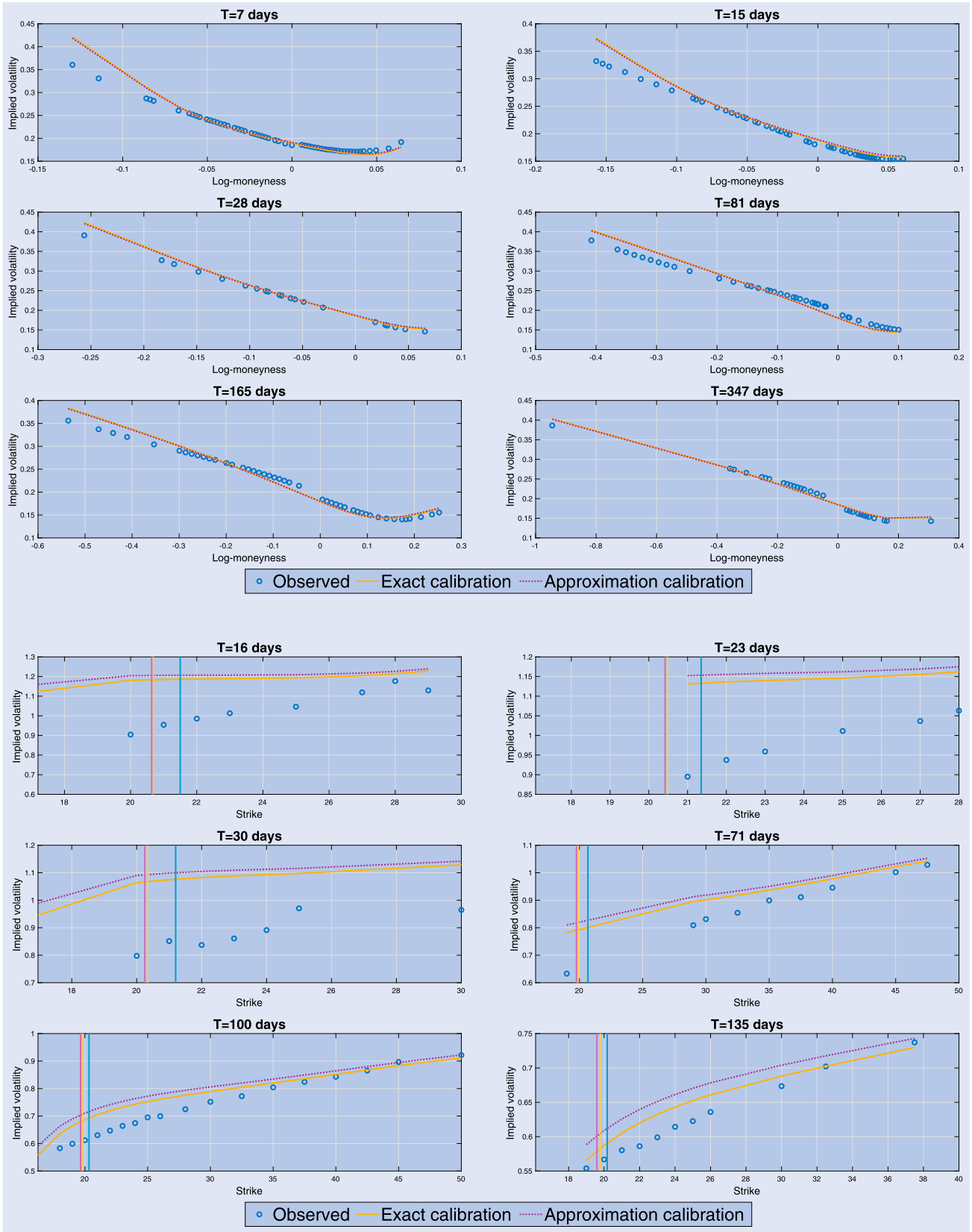

Figure A4. Comparison of SPX implied volatilities on January 7th 2019 between the calibrated approximation and exact pricing formula.

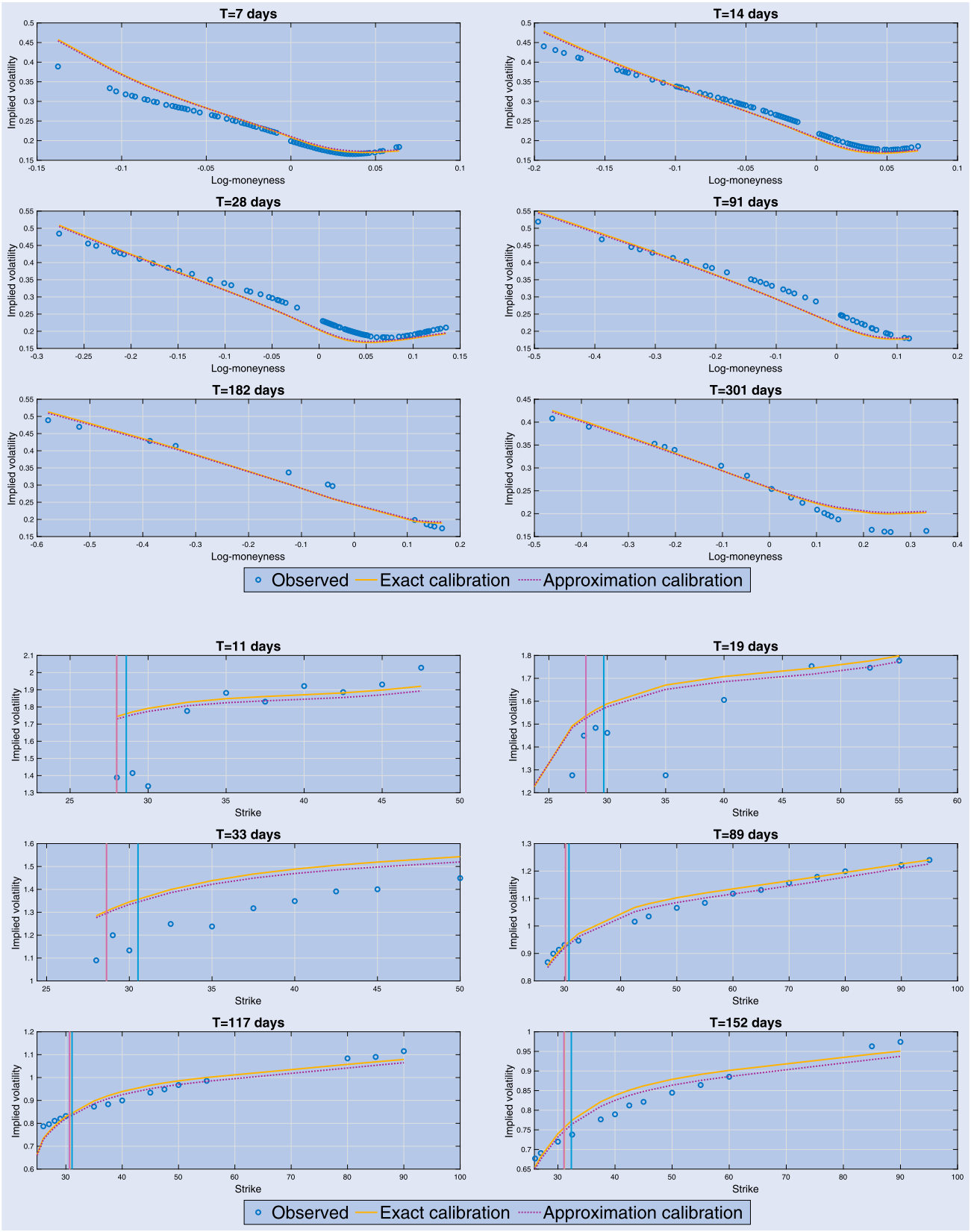

Figure A5. Comparison of SPX implied volatilities on May 22nd 2020 between the calibrated approximation and exact pricing formula.